January 2015

Investigation Of Laminar Convective Heat Transfer And Pressure Drop Of SiO2 Nanofluid In Ducts Of Different Geometries

Sunday Oluwafemi Hassan

Follow this and additional works at: https://commons.und.edu/theses

www.manaraa.com

INVESTIGATION OF LAMINAR CONVECTIVE HEAT TRANSFER AND PRESSURE
DROP OF SiO$_2$ NANOFLUID IN DUCTS OF DIFFERENT GEOMETRIES

by

Sunday Oluwafemi Hassan
Higher National Diploma, Yaba College of Technology, 2008
Bachelor of Engineering, HAMK University of Applied Sciences, 2012

A Thesis
Submitted to the Graduate Faculty

of the

University of North Dakota

in partial fulfillment of the requirements

for the degree of

Master of Science

Grand Forks, North Dakota
May
2015

The Thesis, submitted by Sunday Hassan in partial fulfillment of the requirements for the Degree of Masters of Science from the University of North Dakota, has been read by the Faculty advisory committee under whom the work has been done and is hereby approved.

Clement Tang, 7-May-2015
Dr. Clement Tang, Chairperson

Forrest E. Ames 7 May 2015
Dr. Forrest Ames, Committee Member

N Grewal 7 May 2015
Dr. Nanak Grewal, Committee Member

This thesis is being submitted by the appointed advisory committee as having met all of the requirements of the school of Graduate Studies at the graduate school of the University of North Dakota and is hereby approved.

Wayne Swisher
Dr. Wayne Swisher
Dean of Graduate School

May 7, 2015
Date

PERMISSION

Title	Investigation of Laminar Convective Heat Transfer and Pressure Drop of SiO$_2$ Nanofluid in Ducts of Different Geometries
Department	Mechanical Engineering
Degree	Master of Science

In presenting this thesis in partial fulfillment of the requirements for a graduate degree from the University of North Dakota, I agree that the library of this University shall make it freely available for inspection. I further agree that permission for extensive copying for scholarly purposes may be granted by the professor who supervised my thesis work or, in his absence, by the chairperson of the department or the dean of the Graduate School. It is understood that any copying or publication or other use of this thesis or part thereof for financial gain shall not be allowed without my written permission. It is also understood that due recognition shall be given to me and to the University of North Dakota in any scholarly use which may be made of any material in my thesis.

_____
Sunday O Hassan

05/07/2015
Date

iii

TABLE OF CONTENTS

LIST OF FIGURES

x

LIST OF TABLES

ACKNOWLEDGEMENTS

I would sincerely like to acknowledge the unique privilege given by the University of North Dakota to pursue the Master of Science degree in Mechanical Engineering. I am also grateful to the Mechanical Engineering department for their unceasing support throughout my education at the college of Engineering & Mines.

I would like to thank my advisor Dr. Clement Tang for his constant guidance, and support extended to me for the entire duration of the research project. He has been a dedicated mentor whose constant encouragement and patience helped me complete this project successfully.

I would like to thank the thesis committee members, Dr. Forrest Ames and Dr. Nanak Grewal for their support and co-operation towards the completion of this thesis. Finally, I would like to thank colleagues in the thermal science research group at the University of North Dakota: Sarbotham Pant, Emeke Opute and Mohammed Tanveer Sharif for their invaluable time and input provided during the experiment and for the permission to utilize part of their data in my analysis.

In loving memory of my parents, Mr. & Mrs. Olaonipekun Hassan

ABSTRACT

Engineers are seeking alternatives to conventional heat transfer fluids and in an attempt to improve their thermal transport properties, they added thermally conductive solids into the conventional fluids resulting in a fluid called nanofluid. Nanofluid was suggested as an alternative solution to the problem and many publications reported its potential for heat transfer enhancement. This thesis describes the experimental study of 9.58% by vol. silica/water nanofluid flow through different flow geometries which are circular, hexagonal and rectangular ducts of close hydraulic diameter. The experiments are performed at uniform heat flux condition. The aim of this thesis is to determine experimentally the best duct geometry for optimal thermal performance in nanofluids.

The effect of the cross-section of the flow geometry on the enhancement capability of nanofluid is the focus of this research and four different geometries of relatively equal hydraulic diameters were studied. This study compares the result from the different duct geometries in order to identify the best flow channel for optimal heat transfer using nanofluids. Based on the test data, the thermal performance comparisons are made under three constraints (similar mass flow rate and Reynolds number). It was observed from the comparisons that the rectangular duct showed the highest heat transfer capability through a higher Nusselt number and heat transfer coefficients at for the silica/water nanofluid flow. The circular duct was next to the rectangular duct in thermal performance. There was no significant change in friction factor between the ducts for both water and nanofluid flow.

NOMENCLATURE

D_o	Outside diameter[m]
D_i	Inside diameter [m]
d	Diameter of particle[m]
$\frac{du}{dy}$	Velocity gradient, shear rate $[s^{-1}]$
d_p	Diameter of nanoparticles [nm]
d_N	Diameter of the nanoparticle [nm]
f	Friction factor
f_f	Fanning friction factor
h	Convective heat transfer coefficient $[Wm^{-2}K^{-1}]$
h_x	Convective heat transfer coefficient at distance, x $[Wm^{-2}K^{-1}]$
I	Current supplied [Amp]
k	Thermal conductivity $[Wm^{-1}K^{-1}]$
k_f	Thermal conductivity of the base fluid $[Wm^{-1}K^{-1}]$

L	Length of the test section [m]
$\dot{m}$	Mass flow rate [kg/s]
Nu	Nusselt number
Pr	Prandtl number
Q	Heat/power supplied [W]
q	Heat flux [Wm^{-2}]
Re	Reynolds number
T	Temperature [°C]
T_c	Half of the base fluid boiling temperature [°C]
T_b	Bulk fluid temperature [°C]
$T_{b,out}$	Outlet fluid bulk temperature [°C]
$T_{b,in}$	Inlet fluid bulk temperature [°C]
T_o	Reference temperature [°C]
ΔT	Temperature difference [°C]
V	Voltage supplied [Volts]
ΔV	Voltage drop [Volts]
x	Axial distance [m]

x^+	Dimensionless distance
x_e	Thermal entry length [m]

Greek Symbols

$\partial T/\partial y$	Temperature gradient [Km^{-1}]
η_{nf}	Viscosity of nanofluids [Pa.s]
η_{bf}	Viscosity of base fluid [Pa.s]
μ	Dynamic Viscosity [Pa.s, cP]
ρ	Density [Kgm^{-3}]
τ	Shear stress [Nm^{-2}]

Abbreviations

NF	9.58% volume fraction SiO_2/water nanofluid

CHAPTER I

INTRODUCTION

1.1 Heat Transfer Enhancement

Many engineering systems utilize fluids for their operation for different applications; either as fuel or coolant. One of the critical aspects of practical fluid engineering is the study of heat transfer for fluid flow through ducts under varying conditions such as different fluid velocities, duct geometries, and fluid viscosities at different range of temperatures.

Engineers are seeking an efficient method to remove heat because heat removal is one of the main challenges in numerous industries such as transportation, manufacturing, especially in microelectronics and power generation where enormous heat is usually generated which will adversely affect the device without efficient cooling. The existing cooling methods are inadequate for the high amount of heat required to be removed in some advanced systems like in the microelectronics industries such as microchips which are integral part of computer processors used in everyday life. Many devices use smaller microchips, thereby requiring higher heat flux density and in order to efficiently manage the consequent heat dissipation; an adequate heat transfer method must be employed. It has been estimated that the next generation of computer chips will dissipate a localized heat flux above $10MW/m^2$ (Kaufui & Omar, 2010).

- 1 -

The knowledge of heat transfer applications is required in the design of piping systems and their added components like valves, pumps, fittings etc. for several industrial applications such as cooling in the electronics industries. Heat transfer applications is not only needed at industrial scale, but also for environmental conditioning of private and public buildings which makes it a very important for the wellbeing of the society. Heat transfer is an important process in thermal stations, food pasteurization, ventilating systems etc. which are achieved through some heat transfer devices such as evaporators, condensers and heat exchangers.

Most industrial applications require flow channels that are of different geometries specific to each application which necessitates the need to study the behavior of fluids through ducts of different shapes because this is the reality in the industry compared to the basic circular ducts commonly used in laboratory investigations. Based on the foregoing, it is therefore pertinent to investigate the thermal and flow behavior of heat transfer fluids in ducts of different geometries under varying conditions. One area of focus for this investigation is the study of heat transfer and pressure drop characteristics of the fluids when they flow through different duct geometries which are very useful in many industrial applications. In addition, practical heat transfer systems require an external force from a device such as the pump for the circulation of the working fluid and the associated power consumption can be reduced if the heat transfer fluid is enhanced.

Convective heat transfer processes serve a pivotal role in many industrial and biological systems for cooling applications. Ultimately, engineers seek to maximize heat transfer with minimum input power and system size which is dependent on the type of heat transfer fluid and the system design. Some of the several possible ways to improve the heat transfer efficiency are by the application of vibration to the heat transfer surfaces, usage of microchannels, usage of improved surfaces and by enhancing the inherent thermophysical properties of the heat transfer

2

fluid. It was reported that enhanced surfaces such as fins and microchannels can significantly increase heat transfer rates (Alvarado, et al., 2007).

Interestingly, recent advancements in heat transfer applications seek to optimize benefits, minimize losses by accommodating miniaturization and other cost reduction technologies because consumers desire products that are not only more compact and affordable but also more efficient making heat dissipation a matter of great concern. These growing trends in consumers' demands also require an understanding of fluid behavior through the flow passages of different shapes and sizes to accommodate the different resulting design requirements.

One of the very pertinent industrial applications is cooling; which is a significant technical challenge facing all industries because heat dissipation occur in most devices calling for adequate control in order to keep those devices running efficiently with minimal downtime. Cooling is very important in many industrial operations; ranging from air conditioning, transportation, power generation, microelectronics to refrigeration and can be achieved through the use of heat transfer fluids which are expected to be excellent thermal conductors. A heat transfer fluid could be described as a fluid medium (liquid or gas) which flow around or through a system so that heat can be added or removed from the system at an appropriate transfer rate in order to avoid system breakdown due to overheating. The conventional heat transfer fluids which are in use in the industry for decades are water, air, ethylene glycol and mineral oil which have relatively low thermal conductivities, compared to the higher thermal conductivity of some solids. So, an idea was suggested such that a mixture could be formed between the better thermally conductive solids and the less thermally conductive fluids to improve the thermal conductivity of the resulting mixture.

3

Cooling efficiency is enhanced when a better heat transfer fluid is used for cooling applications and several studies have been conducted in search for an enhanced heat transfer fluid as a means of achieving efficient heat dissipation for increased range of temperature operations and compact designs. The inherent physical properties of the fluid are what determine its suitability and efficiency for different heat transfer applications. In order to evaluate the heat transfer performance of a fluid against conventional fluids, it is necessary to characterize its thermophysical properties and other parameters such as the thermal conductivity, viscosity, pressure drop, and convective heat transfer coefficient.

The conventional fluids are rather inadequate for the emerging industrial cooling needs because they score low on these thermophysical properties. For instance, a fluid having low thermal conductivity will be a poor heat transfer fluid.

Water, the most common liquid coolant, has high heat capacity and low cost which makes it a fluid of choice for its low cost, safety and availability especially when additives such as corrosion inhibitors and antifreeze are added to it. For instance, in low temperature environments where temperature goes to below 0°C, ethylene glycol is added to water to prevent freezing. Also, pure deionized water is used as a coolant in electrical equipment because of its relatively low electrical conductivity and the commonest form of gaseous coolant is air. Hydrogen is also used because of its low density, and high thermal conductivity.

1.2 Introduction to Nanofluids

Some researchers carried out extensive studies on the thermal behavior of particulate solids dispersed in liquids through which they identified an approach for improving the physical properties of fluids such as the final thermal conductivity, viscosity etc. through the addition of

4

solid particles whose average diameter are in micrometers or millimeters, to the already existing traditional fluids in order to produce a more thermally efficient two phase colloid. A higher thermal conductivity is expected since these solid microparticles have better thermal conductivity compared to the base fluids.

Surprisingly, they noted that despite the observed enhancements in the heat transfer, some drawbacks such as particle sedimentation, channel clogging, pressure drop, erosion of flow channels and abrasion of the particles were observed (Rostamani, et al., 2010). A potential reason for this problem could be the poor stability of the suspension which was even more pronounced in very small flow channels such as microchannels and minichannels. This observed drawback limited the practical applications of suspensions of solid microparticles in base fluids for heat transfer applications (Wang, et al., 2003; Keblinski, et al., 2002). Therefore, there is still a continued search for heat transfer fluids that can eliminate or minimize these drawbacks.

Nanotechnology is a branch of technology that deals with manipulation of matter at atomic or molecular level with the purpose of creating superior materials with better properties. This technology has proven very promising in recent years especially in energy and healthcare sectors. The scientific community has experienced some improvements in nanotechnology and modern manufacturing technologies which have imparted the emergence of particles whose sizes are of the order of nanometers (nanoparticles). A nanometer can be described as one billionth of a meter as shown in Figure 1.1. Consequent to the development of Nanotechnology, the idea of suspending these very small nanoparticles in a base liquid for improving thermal conductivity was proposed in 1995 (Choi & Eastman, 1995). These fluids are termed nanofluids, which resulted from the technological advancements in the field of modern nanotechnology and the intense research towards improving the performance of the existing heat transfer fluids.

5
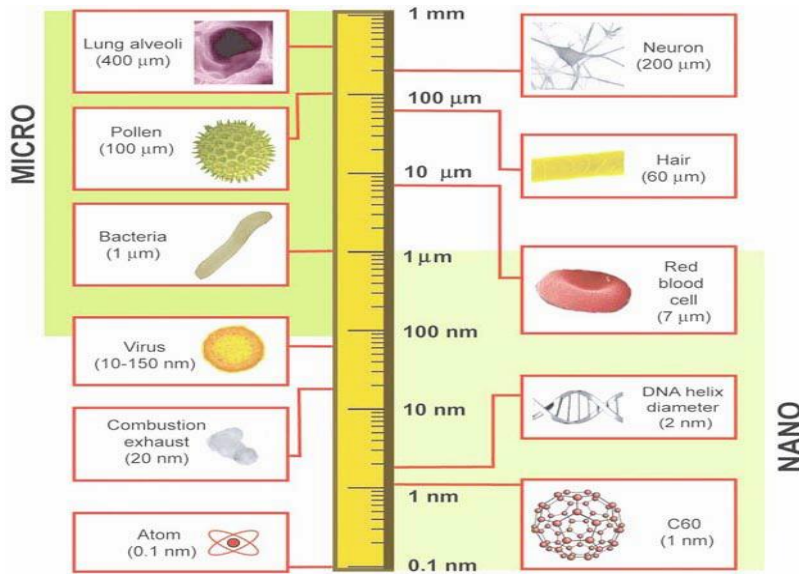
Figure 1.1 Comparison of "nano" and "micro" sizes of many substances (Cristina, et al., 2007).

Nanofluids are engineered colloids which produced by stably dispersing solid nanoparticles in a base fluid. The term nanofluid originated from the team of researchers at the Argonne National Laboratory in Illinois in 1995 (Gireesha & Rudraswamy , 2014; Choi & Eastman, 1995). These researchers discovered that dispersing solid nanoparticles in conventional base fluids such as water, ethylene glycol, mineral oil etc. has the potential of enhancing heat transfer because most of these conventional heat transfer fluids have low thermal conductivities. For instance, the thermal conductivities of water and ethylene glycol at 25°C are 0.58W/m-K and 0.25W/m-K, respectively. In general, the solid particles dissolved in the base fluid include nanofibers, nanotubes, nanowires or nanoparticles.

These solid nanoparticles are mostly metals or oxides of metals such as Al, Cu, SiC, TiC, Ag, TiO_2, Au, SiO_2, and Al_2O_3 which are used for the preparation of the colloids utilized in research and are expected to have high thermal conductivity. Carbon nanotubes (CNT) are also utilized due to their high thermal conductivity ($\approx$ 500W/m-K) in the axial direction. Owing to the high cost of

6

this nanoparticle, metal oxide nanoparticles with thermal conductivity in the range of 10-40W/m-K are used because the thermal conductivity is still two orders of magnitude higher than that of water.

While fine particles have diameters ranging between 100 and 2500 nanometers, nanoparticles are ultrafine particles whose average diameter range between 1 and 100 nanometers (<100nm) implying a very small size. Particles that are as small as 10nm have been used in research (Eastman, et al., 2001). The shape of the nanoparticles usually used in research is spherical but rod-shaped and tube-shaped nanoparticles are also utilized.

The resulting colloids from the dissolution of solid nanoparticles into conventional base fluids is called nanofluid which are much safer to handle as end products compared to their constituent nanoparticles. The main heat transfer enhancement opportunity observed in nanofluids was an abnormal increase in the thermal conductivity and viscosity (Gireesha & Rudraswamy, 2014). According to the literature, nanofluids have better thermophysical properties and is capable of achieving better cooling performance compared to conventional liquids such as water. They were found to exhibit better thermophysical properties compared to the base fluid, such as thermal conductivity, thermal diffusivity and convective heat transfer coefficients (Huaqing, et al., 2011; Yimin & Qiang, 2000; Wei & Huaqing, 2012). Nanofluids are useful in the cooling applications in the industry such as cooling of personal computers, automobile radiators, lubrications, additives for fuels, and other devices. It has been suggested as a cooling fluid in nuclear reactors. The stability of nanoparticles while dispersed in the base fluid are usually improved by adding small amounts of some additives to the mixture.

Many researchers have increased the popularity of the heat transfer capability of nanofluids through extensive research where they investigated the heat transfer performance and flow

7

characteristics of various nanofluids with different nanoparticles and base fluid materials. Through their discovery, nanofluids proved to eliminate some of the demerits of the rather large micrometer-sized particles mainly because of its smaller size which makes it to form better stable suspensions thereby eliminating the existing sedimentation and clogging problems inherent in the use of microparticles. Therefore, nanofluids are better heat transfer fluids especially for microchannels compared to microparticles-based fluids (Chein & Chuang, 2007; Lee & Mudawar, 2007).

Most studies suggested that nanoparticle clustering is of crucial importance for the thermal conductivity enhancement through nanofluids and the sedimentation of the particles can be minimized by using appropriate dispersants. Nanofluids have many potential advantages compared to the suspension of micrometer particles in traditional fluids, some of which are (a) better stability, (b) reduced penalty due to an increase in pressure drop and (c) higher thermal conductivities compared to the suspension of micrometer particles. In addition, it has been suggested that nanofluids are sufficient for cooling the rapid heat dissipation observed in small devices such as the microchips used in computer processors (Lazarus, et al., 2010).

As a result of these advantages, a number of studies have been published on the effective thermal conductivity of nanofluids under macroscopically static conditions and on convective heat transfer of nanofluids. Therefore, nanofluids have some important merits over the conventional colloidal suspensions but studies have reported that its applicability in heat transfer systems is still restricted because of its high viscosity which increases the pumping power.

1.2.1 Production of nanoparticles

8

Broadly speaking, the prominent production methods for nanoparticles are mainly the physical synthesis which comprises processes such as inert-gas condensation technique, mechanical grinding and the chemical synthesis comprising chemical vapor deposition (CVD), micro-emulsions, spray pyrolysis, thermal spraying, and chemical precipitation (Yu, et al., 2008). Manufacturing methods for nanoparticles can also be subdivided into the "bottom up" and "top down" approaches. The bottom up approach relies on growth and self-assembly of single atoms and molecules to form nanostructures which are very useful in creating identical structures with atomic precision while the top down approach relies on disintegrating large-scale material to generate required nanostructures from them which is superior for interconnectivity and integration that is very useful in electronic circuitry.

1.2.2 Production of Nanofluids

On the other hand, nanofluids are also produced through two main two methods (Das, et al., 2007). These methods are: one-step technique and two-step technique. The first step in the two-step technique is the production of nanoparticles and the second step is the scattering of the nanoparticles in a base fluid. The two-step technique is the mostly used method but it suffers from agglomeration of nanoparticles due to strong van der Waals force of attraction thereby preventing the realization of stable nanofluids due to flocculation. One of the advantages of the two-step technique is its appropriateness for mass production of nanofluids nanoparticles especially by utilizing the technique of inert gas condensation for mass production of nanoparticles (Romano, et al., 1997). One of the disadvantages of the two-step technique is the fact that nanoparticle clusters are formed during the preparation of the nanofluid leading to poor dispersion of nanoparticles in the base fluid (Yu, et al., 2008).

Because the quality of the dispersion produced in a nanofluid affects its thermal properties, some physical methods such as stirring and ultrasonication are employed to create stability in the nanofluid but the ability of these methods to produce long term stable dispersions is questionable (see Figure 1.2). Some other chemical techniques such as use of a stabilizing agent and surface treatment on nanoparticles are also used to stabilize the nanofluid.

The one step technique is useful for producing stable nanofluids but it is more expensive. There are some variations of the one-step technique but this technique ultimately combines the production of nanoparticles and the dispersion of nanoparticles in the base fluid into a single step. One of the methods is called the direct evaporation one-step method which involves nanofluid production by the solidification of the nanoparticles, which are initially in gas phase, inside the base fluid (Eastman, et al., 2001). The problem of particle clustering associated with dispersion produced through one-step technique is better than the two-step technique. However, the prominent disadvantage of the one-step technique is that they are not appropriate for commercialization due to their limitation for mass production as a result of the high cost (Yu, et al., 2008).
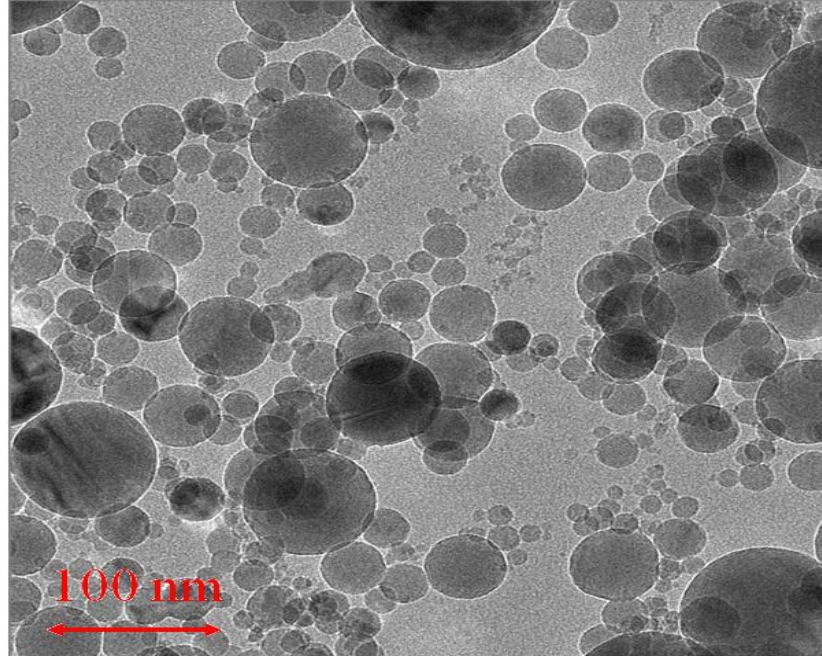
Figure 1.2. TEM image of Al₂O₃/water nanofluid - 0.06% vol. concentration (Sommers, 2012).

In adittion, the properties of the nanofluid used for this experimental investigation are given in the table 1 below:

Table 1

Properties of the SiO₂/water Nanofluid

Nanoparticles	Silicon (IV) oxide
Nanoparticles Conc. by Vol.	9.58%
Color/Odor	Colorless/Odorless
Morphology	Spherical
Density at 20 Celsius	1.2910 g/cm^3
pH	9.51

11

1.3 Thermophysical Properties of the Fluid

In order to adequately characterize the heat transfer and pressure drop behavior along ducts of various geometries, it is important to understand the underlying thermophysical properties of the fluid which are pertinent to understanding the thermal performance and rheology of the fluid. The variation of these thermophysical properties along the ducts under different conditions will help describe the behavior of the fluid especially determine if duct geometry affect the thermal performance of the fluid.

1.3.1 Pressure Drop and Friction Factor

Pressure drop is the difference in pressure between two points of a fluid as it passes through a channel. The drop in pressure results from frictional forces which reduces the flow of the fluid as it passes through the tube. The first thing step in considering pressure drop or pressure loss due to fluid flow in a pipe is to determine the friction between the fluid and the duct. This is often called friction factor and it is then incorporated into pressure loss or fluid flow calculations. Friction factor is not a constant but dimensionless parameter often used to quantify pressure drop in flow applications and it is directly related to the pumping power requirements in flow applications. In other words, low friction factor will imply a low power requirement. In general, pressure drop depends on parameters such as the surface roughness of the pipe which determines friction, vertical pipe difference or elevation, and change in velocity of flow. The key factors affecting the pressure drop as a fluid moves through a duct are Reynolds Number of the fluid and the roughness of the duct (smooth or rough duct).

The famous Darcy–Weisbach equation (named after Henry Darcy and Julius Weisbach) is the equation often used, which relates the head loss or pressure loss due to friction along a given

length of duct to the average velocity of the fluid flow. The pressure loss (ΔP) can be expressed from the Darcy-Weisbach equation as follows:

$$\Delta P = f \frac{L}{D_i} \frac{V^2}{2g} \rho = f_f \frac{L}{D_i} \rho 2V^2 \qquad (1.1)$$

The Darcy–Weisbach friction factor (f) is 4 times the Fanning friction factor (f_f) which was named after Thomas Fanning.

That is, $f = 4f_f$ or $f_f = \frac{f}{4}$ \qquad (1.2)

Fluid flow regimes in industrial applications are mostly turbulent and they have more capacity to enhance heat transfer because of the presence of unsteady vortexes. Hence, there are many studies in the literature on the convective heat transfer of nanofluids in fully-developed turbulent flow regime because they are crucial for practical applications. However, pressure drop information is also essential in order to use nanofluids as heat transfer fluids in industrial applications because it affects pumping power. Researchers have proposed several models for pressure drop of different nanofluids under different flow regime.

Some researchers have proposed a model for predicting the pressure drop of TiO$_2$/water nanofluids in fully developed turbulent flow by using a GA–PNN hybrid system which depends on Reynolds number, nanoparticle volume concentration and average nanoparticle diameter. The GA–PNN hybrid system consists of a neural network and the genetic algorithm part which was used to find the best network weights for minimizing the training error and finding the optimal structure for a GMDH-type polynomial neural network. They compared their results with experimental data points and with other existing correlations through which they concluded that

13

the proposed models are in good agreement with experimental data and show better accuracy with experimental data in comparison with the existing correlations (Meyer, et al., 2013).

1.3.2 Forced Convective Heat Transfer and Nusselt Number

Convective heat transfer is simply heat transfer by convection, which is the most dominant mode of heat transfer in fluids-liquids and gases. Convection is the process by which heat is transferred between a surface and a fluid through the movement of fluids due to density differences caused by temperature variations in the fluid. The application of heat at the boundary layer causes a temperature rise which leads to a reduction in density of the fluid. This change in the density will cause the fluid to rise and be replaced by cooler fluid which will also be heated and rise until the temperature is uniform leading to boiling. For this reason, boiling and condensation are convective heat transfer processes. In reality, convection involves conduction, diffusion and bulk motion of molecules (advection).

Convection may be forced or assisted and natural or free. The later involves movement of fluids and transfer of heat by natural buoyancy forces, which is when the fluid heat transfer happens without the aid of an external source such as fan etc. The forced convection is the direct opposite which happens with the help of an external source of power such as pumps or through thermal expansions. Newton described the heat transfer per unit surface through convection using the equation:

$$q = h_c A dT \tag{1.3}$$

Forced convection heat transfer takes place when a fluid is moving past a solid surface and one of the major parameters for estimating it is the forced convective heat transfer coefficient. Forced convective heat transfer coefficient correlations are often expressed in terms of Nusselt,

Prandtl, and Reynolds numbers. A dimensionless number called Nusselt number is often used to quantify the convective heat transfer. The Nusselt number is the ratio of the convective heat transfer to the conductive heat transfer; which implies that convection is efficient with a high Nusselt and less dominant with a low Nusselt number.

Mathematically, the Nusselt number is written as:

$$Nu_D = \frac{hD}{k} \qquad\qquad (1.4)$$

The evaluation of Nusselt number is dependent on the Reynolds number and the Prandtl number based on the flow regime (laminar or turbulent). A turbulent flow is characterized by a high Nusselt number. For a developing laminar flow, the Nusselt number slowly decreases from a higher value and approaches to a constant value of 4.36 under fully developed conditions for constant heat flux and a value of 3.66 under a fully developed isothermal condition.

1.3.3 Viscosity

Viscosity can be described as a measure of a fluid's resistance to flow; that is; the resistance of a fluid to a change in its shape. It may also be defined as a measure of the internal friction between the molecules of a fluid; such friction opposes the development of velocity differences within a fluid. Therefore, a fluid with is very thick (large viscosity) will resist motion because its molecular makeup gives it a lot of internal friction while a fluid with low viscosity flows easily because its molecular makeup results in very little friction when it is in motion. This internal friction results when layers of fluid slide past each other causing shearing between the layers of fluid. The viscosity of a fluid is a measure of its tendency to resist flow which is the ratio of the shear stress (τ) to the shear rate ($\frac{du}{dy}$). A constant viscosity measurement in any fluid indicates a Newtonian behavior whereas if it varies with shear rate, such a fluid is a non-Newtonian fluid.

15

Viscosity is a major factor in determining the forces that must be overcome when fluids are used in flow applications because it affects the pumping power requirement and the workability of the fluid. Viscosity is measured using a viscometer and the reciprocal of viscosity is called fluidity that is; a measure of the ease of flow. The viscosity of liquids decreases with an increase in temperature while the viscosity of gases increases with an increase in temperature. Thus, upon heating, liquids flow more easily, whereas gases flow more reluctantly. Therefore, viscosity is temperature dependent. The viscosity of a fluid is a measure of its resistance to gradual deformation by shear stress or tensile stress.

Since viscosity is a measure of resistance to the movement of one layer of fluid over another adjacent layer of the fluid, assume that there are two layers of fluid with a distance, dy and velocities u and $(u + du)$ respectively. The viscosity will cause a shear stress (τ) between the fluid layers as the layers move over one another with relative velocity.

Mathematically, $\tau = \mu \dfrac{du}{dy}$ (1.5)

Viscosity is often used as a criterion for classifying fluids as follows:

(i.) Newtonian Fluid

Many fluids are Newtonian which implies that the tangential, or shearing, stress that causes flow is directly proportional to the rate of shear strain, or rate of deformation, that results. Put simply, the shear stress divided by the rate of shear strain is a constant called the dynamic, or absolute, viscosity for a given fluid at a fixed temperature. Hence, a Newtonian fluid is such fluid whose value of viscosity remains constant when the strain rate is varied at a given temperature and some examples of Newtonian fluids are water and air. In a Newtonian fluid, the plot between the shear stress and the shear rate is linear, passing through the origin.

16

(ii.) Non-Newtonian fluid

A non-Newtonian fluid is the opposite of Newtonian fluid whose value of viscosity changes with the variation of the strain rate at a given temperature. This means that when the strain rate is varied, the shear stress does not change in the same proportion at a given temperature. Non-Newtonian fluids are classified based on the variation of their viscosities, however, viscosities is not sufficient to describe the mechanical behavior of a non-Newtonian fluid. There is a need for a more extensive understanding of other properties to better articulate their rheological behavior. In general, non-Newtonian fluids are called pseudoplastic (shear thinning behavior), if they show a decreasing viscosity while the strain rate is increasing, and if they exhibit an increasing viscosity while the strain rate is increasing, they are called dilatant (shear thickening behavior). It is worthy of note that nanofluids can behave as both Newtonian and Non-Newtonian fluids under different conditions. In a non-Newtonian fluid, the relationship between the shear stress and the shear rate is non-linear, and can sometimes be time-dependent.

1.3.4 Thermal Conductivity

In order to describe heat transfer in any material, the thermal conductivity of such material must be considered. In fact, the rate of heat transfer in a material depends on the temperature gradient and the thermal conductivity of the material. Thermal conductivity therefore, is the property of the material to conduct heat. It is primarily expressed in Fourier's Law for heat conduction and its unit is watts per kelvin-meter. The reciprocal of thermal conductivity is thermal resistivity.

In mathematical terms, Fourier's law for heat conduction is as follows:

$$\frac{Q}{A} = k \frac{dT}{dy} \tag{1.6}$$

17

From the above equation, we can infer that thermal conductivity depend on the heat flow per unit area and the temperature gradient. Some other factors that can influence the thermal conductivity of a material are the structure of the material, composition of the material and phase change of materials. The value of thermal conductivity of a material will significantly affect the heat transfer rate. For instance, a material of higher thermal conductivity will transfer heat faster than that of a lower thermal conductivity. For this reason, materials of higher thermal conductivity are used in heating and cooling applications while materials with lower thermal conductivity are used for insulation applications.

1.4 Objectives of the Research

The use of nanofluids for enhancing heat transfer is attractive in a range of applications. Some studies have shown that with a relatively higher enhancements in thermal properties of heat transfer fluid, the potential for enhancement in heat transfer applications is considerable and extensive studies on the enhancements in convective heat transfer and pressure drop characteristics of nanofluids are available in literature. However, these results have not been experimentally compared for different flow geometries based on available literatures.

The main objective of this research is the investigation and comparison of the forced convective heat transfer and pressured drop characteristics of aqueous suspensions of 9.58% by volume concentration SiO_2/water nanofluid in ducts of different geometries. The ducts geometries considered are rectangular, square, hexagonal and circular of comparable sizes, with the hydraulic diameters being the basis for comparison. The experimental results from each geometry was analyzed and compared with one another. The SiO_2/water nanofluid was characterized by measuring the thermophysical properties from which the pressure drops and heat transfer behavior were studied.

18

The experimental set up and methodology was validated using distilled water and the result was compared with existing result from literature. After the validation using distilled water, the SiO_2/water nanofluid was then passed through the different geometries. Some of the goals of this research is to find out if the duct geometry affects the heat transfer enhancement capability of the NF, measure the friction factors and convective heat transfer coefficient of the NF over a range of Reynolds number covering the laminar, transition and the early stage of turbulent regime.

The motivations for this research are: (a) little work was found from literature that compares the convective heat transfer characteristics of SiO_2/water nanofluid through flow channels of various geometries; (b) little work was found in literature on the pressure drop characteristics of SiO_2/water nanofluid in ducts of various geometries and, (c) some inconsistencies from the reported results on the pressure drop convective heat transfer characteristics of SiO_2/water nanofluid.

1.5 Structure of the Thesis

The rest of the thesis is as follows:

Chapter II comprises a detailed review of literature from various sources regarding experimental and theoretical studies on the pressure drop characteristics, thermal conductivity, and convective heat transfer characteristics of nanofluids.

Chapter III discusses the experimental setup, experimental procedure and the uncertainty associated with the measurements.

Chapter IV discusses the validation of the experimental procedure through experimental results of distilled water, presents the experimental results on pressure drop and convective heat transfer of the nanofluid, and compares the results with established correlations.

19

Chapter V comprises summary of the research, important conclusions, and some recommendations for future work.

CHAPTER II

LITERATURE REVIEW

The continued search for super-efficient and energy-saving heat transfer fluid has opened a world of opportunities for research towards discovering new working fluids of better thermal properties which is useful under different conditions. This quest led to the discovery of nanofluids which contain solid particles whose characteristic size is less than 100 nm. This increasing demand for high thermally conductive working fluid has generated a lot of publications focused on the characterization of the thermophysical properties of several nanofluids such as Nusselt number, effective viscosity, effective thermal conductivity, thermal diffusivity, specific heat capacity, Prandtl number, and so forth, with which researchers investigate the convective heat transfer and pressure drop characteristics of nanofluids (Wang, et al., 2009; Wang, et al., 2009).

Many publications resonated the fact that increasing the thermal conductivity of base fluids by suspending nanoparticles in them would enhance the convective heat transfer coefficient, viscosity and the effective thermal conductivity of the base fluid because solids generally have inherent high thermal conductivity which will eventually enhance heat transfer (Salman, et al., 2014). Although the degree of enhancement through thermal conductivity continues to be a matter of debate amongst different research groups, little research was performed on the potential effect of flow passage geometry on heat transfer enhancement. Basically, very little literature was found on the impact of duct geometry on heat transfer enhancement with nanofluid as the working fluid. The literature available on nanofluids is huge and varied but for the sake of this research, the

21

review will be focused on the aspects relevant to the thermal conductivity, pressure drop and heat transfer performance of nanofluids.

2.1 Convective Heat Transfer of Nanofluids

A survey of the thermal properties of many liquid coolants available today for heat transfer applications showed a rather poor thermal conductivity compared to the higher thermal conductivities of solid metals and based on the emerging needs, better heat transfer fluids are being sought (Rostamani, et al., 2010). Several studies have been conducted to investigate convective heat transfer of nanofluids and over 1000 published research works on the opportunities of nanofluids for heat transfer enhancement are growing over the last decade (Haghighi, et al., 2014). A good amount of research have been focused on the reported higher thermal conductivity of nanofluids compared to traditional fluids and many fluid engineers have made efforts to increase the thermal conduction of the cooling fluid through certain techniques such as agitation, increase in surface area, or addition of solid particles but this yielded limited improvement for base fluids of very inherent low thermal conductivity. Therefore, it is necessary to find an effective method to improve the thermal conductivity of the base fluid (Rostamani, et al., 2010).

The idea of adding solid nanoparticles to the base fluid with the hope of increasing the thermal conductivity of the resulting fluid mixture has received a lot of attention evident in many literatures. There is still some disagreement in the literature about the claims of the research groups regarding whether nanofluids show unusual thermal properties caused by dispersing little amount of nanoparticles in a base fluid resulting in drastic increase in thermal conductivity and heat transfer coefficients of the nanofluid (Hwang, et al., 2009; Anoop, et al., 2009; Wen & Ding, 2004). Most of these published works show the capacity of nanofluids to enhance the parameter that cause heat transfer in fluids.

22

For instance, through a numerical investigation of turbulent forced convection flow of CuO/water, TiO$_2$/water and Al$_2$O$_3$/water nanofluid mixture with different volume concentrations of nanoparticles in a long horizontal duct while varying different properties under constant heat flux condition, it was found that the shear stress, the Nusselt number and the heat transfer coefficient of the nanofluids are strongly dependent on the volume concentration of nanoparticles and these thermophysical properties increase by increasing the volume concentration of nanoparticles (Rostamani, et al., 2010).

For this particular study, the nanofluid used is a mixture of water as the base fluid with the three different nanoparticles are dispersed in it at different concentration ranging from 0 to 6% by volume. The standard $k - \varepsilon$ turbulence model was used to predict the kinetic energy and the dissipation rate in the turbulent flow and the Reynolds number at the inlet was varied from 20,000 to 100,000. The base fluid was water and all the thermophysical properties of nanofluid mixture are temperature-dependent. The Nusselt numbers predicted for each of the nanofluid was in good agreement with other well-established correlations such as the Gnielinski correlation (see Figure 2.2) and could be used to predict the heat transfer behavior of nanofluids (Rostamani, et al., 2010).

In addition, Rostamani, et al., (2010) validated their model using water in the turbulent regime by comparing the Darcy friction factor and the Blasius correlation with theoretical result from which they observed a good agreement (see Figure 2.1) which proved that the numerical procedure was reliable for predicting turbulent forced convection flow in a horizontal duct. They observed that the effect of CuO nanoparticles to enhance the Nusselt number is better than Al$_2$O$_3$ and TiO$_2$ nanoparticles under constant volume concentration of the nanoparticles and constant Reynolds number. In addition, the viscosity of the nanofluids was obtained from experimental data (Rostamani, et al., 2010).

23
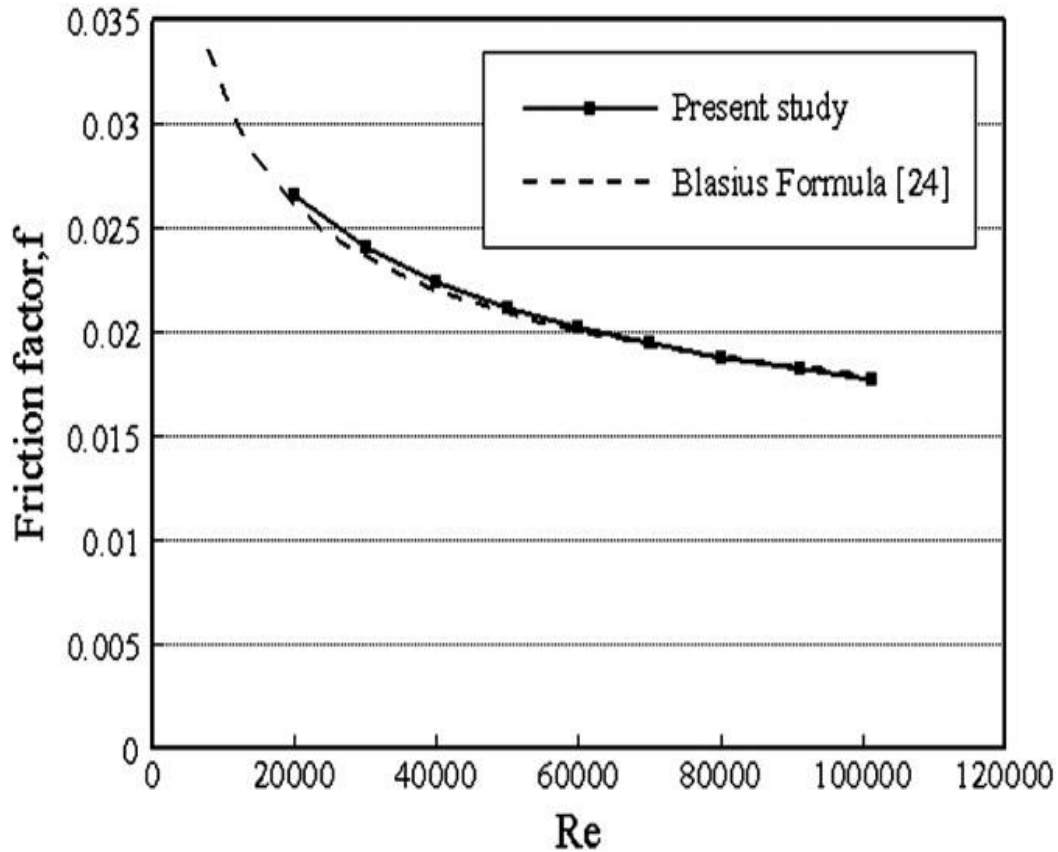
Figure 2.1 Comparison of the Darcy friction factor and the Blasius formula against the computed values for water in turbulent regime (Rostamani, et al., 2010).

Very recently, Haghighi, et al., (2014) experimentally studied the convective heat transfer coefficients of 9wt% Al_2O_3-water and 9wt% TiO_2-water nanofluids inside pipe circular tubes under turbulent flow with constant heat flux at the walls and specifically discussed methods of comparing the performance of these two nanofluids. The experimental investigation was carried out independently by the Royal Institute of Technology, KTH (Sweden) and the University of Birmingham (UK) whose experimental data agreed very well. From their results, the experimental data indicated that Nusselt numbers and friction factors of the nanofluids are well correlated by the equations developed for single phase fluids within a margin of 20% and 10% respectively.

24

These result validated the assumption that heat transfer and pressure drops of nanofluids can be predicted satisfactorily by using conventional correlations developed for single phase fluids.

Interestingly, the authors noted that the idea of comparing the thermal performance of nanofluid at equal Reynolds number with a focus on the viscosity is not practically relevant because heat transfer can always be increased by increasing the flow rate; implying that equal pumping power is a better basis for comparison because it accounts for the total cost of removing the heat from the system (pumping cost). Surprisingly, this method of comparison is still used in the literature (Mojarrad, et al., 2014; Abreu, et al., 2014; Sundar, et al., 2014; Ebrahimi, et al., 2014). In addition, it was observed that, at equal pumping power, the heat transfer coefficient of Al_2O_3 nanofluid was the same as that of water while that of TiO_2 was about 10% lower. Finally, they concluded that both nanofluids did not show any benefit for cooling applications in turbulent flow since the increases in viscosities were higher than the enhancements of heat transfer coefficient thereby requiring higher pumping power.

In an experimental investigation, Yimin & Qiang (2003) studied the characterization of a Cu-water nanofluid which flows through a straight tube with a constant heat flux under both laminar and turbulent flow conditions. They reported that the suspended nanoparticles significantly enhanced the heat transfer performance of the traditional base fluid and their friction factor agreed well with that of the water. In addition, they proposed new convective heat transfer correlations for prediction of the heat transfer coefficients of the nanofluid for both laminar and turbulent flow conditions. It was reported that the dispersion of solid nanoparticles in traditional fluids changes their thermal conductivity and viscosity. Moreover, due to less pressure drop in noncircular ducts, the heat transfer rates through them is smaller compared to that of circular tubes and consequently the addition of nanoparticles to traditional heat transfer fluids may enhance heat

25

transfer properties of noncircular ducts. A new correlation was proposed which accounts for the microconvection and microdiffusion effects of the suspended nanoparticles.

However, the authors observed that the Dittus-Boelter correlation could not predict the dependency of the Nusselt number of the nanofluid on the volume fraction of nanoparticles because of its validity for only single-phase flow especially when the volume fraction of the nanoparticles is larger than 0.5 percent. In addition, they reported that the friction factor for the dilute Cu-water nanofluids is approximately the same as that of water so that the low volume fraction of the suspended nanoparticles does not lead to additional penalty of pump power.

Majority of the published works on nanofluid heat transfer enhancement centered on flow through circular ducts. However, it is equally important to investigate the convective heat transfer and flow behavior of nanofluid through noncircular ducts because noncircular ducts such as hexagonal, rectangle, and square geometries are prevalent in many industrial heat transfer applications especially towards the realization of a more compact heat exchanger. It was reported that an increased effort is being directed at saving costs of energy, material and labor by producing a more efficient heat exchanger because heat transfer enhancement depend on fluid performance and the cost of manufacturing (Kakac, et al., 1981). As a result, ducts of varied geometries will experience increased utilization for heat transfer applications. Some analytical solutions of heat transfer and pressure drop for laminar flows in different duct geometries are available in the literature (Shah & London, 1978).

In order to assess the impact of duct geometries on losses during heat transfer, an investigation was performed to determine the optimum duct geometry that minimizes losses by comparing the entropy generation and pumping power for a range of laminar flows and constant heat flux. The duct geometries considered are circular, square, equilaterally triangular, rectangular

26

with an aspect ratio of 1/2 and sinusoidal with an aspect ratio of $\sqrt{3}/2$. From the result, it was observed that the circular geometry is the best, especially when the frictional contributions of entropy generation becomes critical and the triangular and rectangular duct geometries are not good choices for both entropy generation and pumping power. The hydraulic diameters were used for the different geometries since they are noncircular (Sahin, 1998).

An aqueous solution of various-sized gold nanoparticles, that is, gold-deionized/water nanofluid flowing through a conventional heat pipe of a diameter 6 mm and length 170 mm was investigated for heat transfer performance. From the result, it was deduced that the nanofluid causes a significant reduction in the thermal resistance of the heat pipe compared with only deionized water at given concentrations. Furthermore, the thermal resistance of the heat pipes for the nanofluid was lower than that of water which implies that the higher thermal performances of the nanofluid have proved its potential as a substitute for conventional water in vertical circular meshed heat pipe. Hence, the addition of gold was significant for heat transfer enhancement (Tsai, et al., 2004).

In a numerical investigation, Jahanshahi, et al. (2010) studied the effect of SiO_2 nanoparticle on heat transfer in a square cavity whose volume fraction of nanoparticle are between 0 and 4% and Rayleigh number of water between 10^5 and 10^7, subject to different side wall temperatures. The thermal conductivity of the nanofluid was measured experimentally. Their result showed that increasing the nanoparticle concentration for the range of Rayleigh numbers causes an observable enhancement in the local Nusselt number and heat transfer. In addition, it was observed that the heat transfer increases by increasing the Rayleigh number for a particular volume fraction.

27

Through an experimental study, Pak & Cho (1998) observed and analyzed the convective heat transfer and the friction factor in the turbulent flow regime using Al_2O_3 and TiO_2 nanoparticles dispersed in water. From their result, they concluded that the effect of Reynolds number on the heat transfer enhancement was negligible and the Nusselt number of the nanofluids increased with increasing volume fraction of the suspended nanoparticles.

In an experimental investigation of the convective heat transfer coefficient of Al_2O_3/water and CuO/water nanofluids at different concentrations for laminar flow through circular tube under a constant wall temperature boundary condition, the results showed that the single phase correlation for thermophysical properties is not sufficient to predict heat transfer enhancement of nanofluids. Also, the experimental results showed that heat transfer coefficient increases with increasing nanoparticles concentrations and increasing Peclet number for both nanofluids. However, the Al_2O_3-water nanofluids showed greater enhancement compared with CuO-water and the convective heat transfer coefficient of pure water increased to 41% and 38% at 3% volume concentration of Al_2O_3 and CuO nanoparticles respectively (Heris, et al., 2006).

An experimental study of heat transfer on Al_2O_3-water nanofluid flowing through a copper tube in laminar flow under constant wall heat flux, Wen & Ding (2004) observed an increase in nanofluid heat transfer coefficient with Reynolds number and nanoparticles concentration particularly at the entrance region and it decreases with axial distance. Also, it was shown that the classical Shah correlation was insufficient to predict the heat transfer behavior of nanofluids. However, they suggested that the enhancement of the convective heat transfer could not be only attributed to the enhancement of the effective thermal conductivity and one possible reason identified for the enhancement was migration of nanoparticles which could cause a non-uniform

28

distribution of thermal conductivity and viscosity field and a resulting reduction and disturbance of the boundary layer thickness.

A numerical study on forced convection flow of Al_2O_3-water and Al_2O_3-ethylene glycol nanofluids inside a uniformly heated circular tube subject to a constant heat flux boundary condition (50W/cm^2) on its wall was carried out by a group of researchers. The result showed that the presence of nanoparticles significantly increased the heat transfer at the tube wall for both the laminar and turbulent regimes which was even more significant with increasing particle concentration. In contrast, this addition of nanoparticles had an adverse effects on the wall friction (wall shear stress) which is more pronounced for the Al_2O_3-ethylene glycol nanofluid with increasing particle concentration. The results also indicated that the Al_2O_3-ethylene glycol nanofluid gives a better heat transfer enhancement than the Al_2O_3-water mixture. From the study, they derived a new correlation for the Nusselt number (Maiga, et al., 2004).

Some researchers conducted an experiment through which they studied the heat transfer and flow behavior of TiO_2-water nanofluid flowing in an upward direction through a vertical pipe in both the laminar and turbulent flow regimes under a constant heat flux boundary condition. The observed results depicted that the convective heat transfer coefficient increased with an increase in nanoparticle concentration in both the laminar and turbulent flow regimes at a given Reynolds number and particle size (He., et al., 2007).

A research was conducted on the application of aluminum oxide nanofluid in diesel electric generator as jacket water coolant through which they demonstrated that owing to the better convective heat transfer coefficient of the nanofluid, the efficiency of waste heat recovery heat exchanger increased (Kulkarni, et al., 2008). Many published works on nanofluid heat transfer properties and enhancement centered on flow through circular ducts but it is important to equally

investigate the convective heat transfer properties of nanofluids through noncircular ducts as well because noncircular ducts (hexagonal, rectangle, square etc.) are prevalent in many industrial heat transfer applications especially in compact heat exchangers (Sahin, 1998).

An investigation into the heat transfer enhancement and the behavior of the Al_2O_3-water nanofluid flowing under a turbulent flow regime inside the cooling system of microprocessors or other electronic components was carried out. Their results showed that the nanofluid gave a larger heat transfer coefficient than the base fluid and that the nanofluid with smaller particle diameter provided a higher heat transfer coefficient (Nguyen, et al., 2007).

An experimental investigation into the heat transfer capability of CuO/deionized-water nanofluid as it flow through copper tube under laminar flow was performed. Their results showed that the heat transfer enhancement was increased considerably as the Reynolds number increased and they reported 8% enhancement of the convective heat transfer coefficient of the nanofluid at 0.003% volume concentration of CuO nanoparticles (Asirvatham, et al., 2009).

In an experimental investigation, Liu et al., (2007) studied the forced convective heat transfer characteristics by passing deionized water through quartz microtubes of inner diameters of 242, 315 and 520μm for Reynolds number ranging from 100 to 7000. From their results, an agreement between the experimental Nusselt number and the laminar correlations when the flow state was laminar was observed. Through a numerical investigation, Lelea (2010) studied the effects of temperature dependent thermal conductivity on Nusselt number behavior in stainless steel microtubes using three different fluids which has temperature dependent fluid properties under laminar flow. The microtube has a diameter ratio of $D_i/D_o = 0.1/0.3$ mm and a tube length of 70 mm. The Reynolds number range was less than 400. From their results, they inferred that

provided the Reynolds number was kept low, the thermal conductivity has a significant influence on the behavior of the local Nusselt number.

An investigation on nanoparticles within conventional phase change materials such as water was performed by some researchers. Their findings show that nanoenhanced phase change material (NEPCM) has great potential for demanding thermal energy storage applications (Khodadadi & Hosseinizadeh, 2007). An experimental study on the turbulent convective heat transfer and pressure drop of dilute CuO/water nanofluid inside a circular tube was performed and it was reported that the convective heat transfer coefficient was enhanced by 25% at a low concentration of copper oxide between 0.015% and 0.236% volume fractions (Fotukian & Esfahany, 2010). In a numerical study of the heat transfer of turbulent flow of CuO, Al_2O_3, SiO_2 nanoparticles with ethylene glycol and water as base fluids with different volume concentration flowing in a tube under constant heat flux condition. They measured the nanofluid viscosity and developed correlations for the nanofluid viscosity as a function of temperature up to 10% of volume concentration. From their results, it was observed that the heat transfer coefficient increases with increasing volume concentration of the nanoparticles (Namburu, et al., 2009).

In a numerical study, the effect due to the uncertainty in the values of the physical properties of Al_2O_3/water nanofluid on their thermohydraulic performance for laminar fully developed forced convection in a two zone tube was studied. The results revealed that the heat transfer coefficient of Al_2O_3/water nanofluid is increased by 3.4–27.8% under a fixed Reynolds number compared with that of pure water (Minea, 2013). Some authors presented a numerical study of Al_2O_3/water nanofluid with a two-phase Eulerian model and compared with single- and two-phase model. They showed that the new model which was implemented by them gave rise to

31

more accurate results. In addition to the studies on the thermophysical properties, nanofluids have been developed to improve the mass transfer performance in thermal systems (Lotfi, et al., 2010).

Some of the passive conventional methods used to enhance the heat transfer rate includes extended or rough surfaces, swirl flow, and active techniques with surface or fluid vibration and mechanical aids (Webb & Kim, 2005). Enhanced surfaces are employed in thermosystems to enhance the heat transfer rate and this is possible because the thermal conductivities of the solid phases are comparatively greater than that of the working fluids such as water, ethylene glycol etc. Most solids have higher thermal properties compared to the traditional working fluids; hence, which is the basis for adding solid additives to the conventional fluids as a means of enhancing the heat transfer performance of the traditional fluid. This research approach is in high demand (Liu, et al., 2006; Visinee & Somchai, 2010). These metallic or nonmetallic particles are added so that they can change the transport properties and heat transfer characteristics of the base fluid.

Before the introduction of the nanoparticles to this application, microparticles were used for heat transfer enhancement but due to their size, they had the disadvantage of settling quickly, clogging flow channels, eroding pipelines and causing severe pressure drops which could damage the pipe over time (Li & Xuan, 2002). Nanoparticles on the other hand is devoid of that problem because they operate based on Brownian motion which keeps them permanently suspended and when they are in equilibrium with no flow, they are distributed in a balance between buoyant force and thermal agitation. The contribution of Brownian motion of the nanoparticles to the overall thermal conductivity of the nanofluid is very crucial.

At the Argonne National Laboratory, it was the first discovered by a scientist who identified and demonstrated the special ability of this class of fluid which he called nanofluids; a fluid that he presented as having the capability to significantly improve the total heat transfer

32

coefficient of the fluid and augment the amount of heat transported or transferred in various thermal systems (Choi & Eastman, 1995). Nanofluids are colloidal suspensions, i.e., a unique class of nanometer-sized [<100nm] particles of high thermal properties dispersed in a base fluid such as water or ethylene glycol which has the capacity to enhance the thermal properties of the base fluid (Eastman, et al., 1996; Guo, et al., 2010). The last few years have witnessed a rapid growth in published papers on the applications of nanofluids especially in the transportation sector (engine cooling/vehicle thermal management), electronics cooling, enhanced oil recovery, nuclear systems cooling, heat exchanger, biomedicine, drilling fluids etc. (Sommers & Yerkes, 2010; Visinee & Somchai, 2010).

Nanofluids are very promising as the next-generation heat transfer fluids as they offer exciting opportunities for heat transfer enhancement compared to the traditional fluids and their successful employment will aid the current trend towards component miniaturization by enabling the design of smaller and lighter heat exchanger systems (Wang & Mujumdar, 2007). Some common examples of nanofluids are the alumina and silica nanofluids and their enhanced thermophysical properties are due to the larger surface area and the thermal conductivity of the solid nanoparticles dispersed in the base fluid. They have some unique characteristics; some of which are better thermophysical properties, long lifetime and low toxicity that contribute to their heat transfer enhancement capabilities.

The three different approaches used by several research groups to study the behavior of nanofluids are:

- Experimental: achieved by investigating their thermal properties and heat transfer correlations;

33

- Empirical: through the investigation of their thermal properties and similarity solutions;

- Numerical: by single phase and two phase approaches.

However, there are more published results from experimental investigation compared to the empirical and numerical approaches (Das, et al., 2007). Some of the early attempts to numerically explain the behavior of nanofluids made use of the famous Maxwell model for statistically homogenous, isotropic composite materials with randomly dispersed spherical materials. Since the Maxwell model is more applicable to micro particles, its prediction for nanoparticles does not agree with experimental results. However, in order to improve the predictability of nanofluids, Hamilton and Crosser modified the Maxwell's model to accommodate non-spherical particles which is the model widely in use today (Hamilton & Crosser, 1962).

The heat transport properties of nanofluids have been experimentally discovered to depend on the type, the size, the concentration, the shape and the thermal conductivity of the suspended particles, the conductivity of the base fluid and temperature (Wang & Mujumdar, 2007). Small concentrations of nanoparticles dispersed in base liquids have been found to significantly increase the thermal conductivity of the base fluids (Choi, et al., 2001; Das, et al., 2003; Ding, et al., 2006; He., et al., 2007). The enhancement of forced laminar-flow was more significant at the entrance region and an increase in the convective heat transfer coefficient was also observed (Heris, et al., 2007; Pak & Cho, 1998).

The following are some of the factors that could contribute to the heat transfer enhancement capability of nanofluids when compared to solid-liquid suspensions for heat transfer intensifications:

- greater specific surface area and hence, heat transfer between particles and base fluid;

34

- lower pumping power required to achieve the equivalent heat transfer in traditional fluids;

- higher stability of the colloidal suspensions;

- higher level of control of the transport properties through a variation of particle size, concentration, shape to suit different applications;

- Reduced particle clogging compared to conventional slurries.

The technical community holds varying views about the methods used to experimentally investigate the thermal conductivity of nanofluids and several other factors such as poor characterization of suspensions, lack of agreement between results, and the lack of theoretical understanding which have limited the utilization of nanofluids for industrial applications (Kwak & Kim, 2005; Keblinski, et al., 2002; Sommers, 2012). There's still a differing view about the cause of the significant heat transfer since the reasons identified which are Brownian motion, liquid-solid interface layer and surface charge state have not satisfactorily explained the anomalous behavior of the nanofluids. In a recent publication, particle clustering was identified as the reason for the significant thermal properties of nanofluids (Pawel, et al., 2005).

Some of the possible reasons why there is no universally acceptable theory on the behavior of nanofluids could be:

- The thermal behavior of nanofluids does not conform to the already established solid-solid particle interaction. For instance, the thermal conductivity for a solid-solid interaction should reduce with decreasing grain size but it was observed to increase in nanofluids.

- A multidisciplinary approach which involve knowledge of material science, physics, chemistry etc. is necessary in order to understand the unique behavior of nanofluids and their performance.

35

Published works in the nanofluids research area have established the fact that nanofluids enhance heat transfer but this behavior was observed at high concentration of the nanoparticles. Their high viscosity is a concern yet to be exhaustively considered against the viscosity of conventional fluids and the heat transfer enhancement was observed to be particularly significant at the entrance region. It is pertinent to validate the trade-offs between the use of nanofluids and conventional fluids for heat transfer enhancements. The characterization of the heat transfer rate as the fluid is forcefully pushed through these ducts will be measured but we need to quantify how it differs compared to water as the traditional fluid. The rheological analyses of nanofluids have shown that they can exhibit both Newtonian and non-Newtonian behavior depending on factors such as particle concentration, particle size and shape and viscosity of the base fluid etc.

2.2 Pressure Drops Characteristics of Nanofluids

The experimental investigation of the convective heat transfer and pressure drop of water-based Al_2O_3 nanofluids under laminar fully developed flow regime was carried out. From the experimental data, two correlations was proposed for calculating the thermal conductivity and dynamic viscosity of nanofluids as a function of temperature as well as nanoparticle volume fraction. They also observed that the pressure loss for the nanofluids was about 5.7 times higher than that of pure water and the pressure drop of the nanofluid increased with increasing the volume fraction of nanoparticles. They measure all the physical properties required to calculate the convective heat transfer and the pressure drop and concluded that the Al_2O_3 nanofluids incur large penalty in pressure drop in the laminar flow regime (Heyhat, et al., 2013).

Some researchers performed an experimental study of the convective heat transfer and pressure drop of turbulent flow of TiO_2-water nanofluid through a uniformly heated horizontal circular tube. The nanofluid was prepared by dispersing spherical TiO_2 nanoparticles of 15 nm

36

nominal diameter in distilled water to form stable suspensions. Their results showed that heat transfer coefficients in unaffected by a change in the Reynolds number but increases with increasing the nanofluid volume fraction (Kayhani, et al., 2012).

2.3 Thermal Conductivity and Viscosity of Nanofluids

The thermal conductivity of Al_2O_3 and CuO nanofluids with water and ethylene glycol as the base fluids were experimentally investigated by a group of researchers. Their thermal conductivities were measured by a transient hot-wire method and they observed that thermal conductivity of the nanofluids did not only depend on the shape of the nanoparticle but also the size of the nanoparticles. The experimental results show that these nanofluids have substantially higher thermal conductivities compared to the base fluids. They compared the result from experiment with the numerical model (Hamilton and Crosser) from which they observed that the model can predict the thermal conductivity of nanofluids containing large agglomerated particles (Lee, et al., 1999).

In an experimental research, (Jeong, et al., 2013) investigated under different nanoparticle volume concentrations ranging from 0.05% to 5.0 vol. %, the effect of the shape of nanoparticle on the viscosity and thermal conductivity of ZnO-water nanofluids. Their result showed that the viscosity of the nanofluids increased with corresponding increase in the volume concentration by up to 68.6% for both the nearly rectangular and spherically shaped nanoparticles. The enhancement of the viscosity of the nearly rectangular shape nanoparticles was greater than that of the spherical nanoparticles by 7.7%. In addition, the thermal conductivity of the nanofluids increased for both shapes of the nanoparticles compared to that of the base fluid. The author stated that one possible reason for the observed difference in viscosity and thermal conductivity of the nanofluid in comparison with the base fluid can be attributed to the effective aggregate radius of the nanofluid

37

for each of the nanoparticles. From these results, it was concluded that the shape of the particles has a significant effect on the viscosity and thermal conductivity enhancements of nanofluids.

An experimental investigation on TiO_2 nanoparticles, with spherical and rod-like shapes and dispersed in deionized water for the purpose of assessing the heat transfer performance on the basis of thermal conductivity of the resulting nanofluid, was performed by some researchers. Their result indicated that both the nanoparticle size and shape have effects on the enhancement of thermal conductivity (Murshed, et al., 2005).

Through an experiment investigation on the thermal conductivity of three nanofluids comprising: Al_2O_3, CuO, and ZnO nanoparticles dispersed in a base fluid of 3:2 (by mass) ethylene glycol and water mixture. The particle volumetric concentration tested was up to 10% and the temperature range of the experiment was from 298 to 363K. The results indicated that the thermal conductivity of the nanofluids was enhanced with increases in the volumetric concentration of the nanoparticles and the thermal conductivity increased substantially with increase in temperature. In addition, they compared the experimental data with existing models for thermal conductivity from which they observed a poor agreement. Consequently, a new model was developed which is a modification of an existing model, incorporating the classical Maxwell model and the Brownian motion effect to account for the thermal conductivity of nanofluids as a function of temperature, particle volumetric concentration, the properties of nanoparticles, and the base fluid, which agrees well with the experimental data (Vajjha & Das, 2009).

According to an experiment conducted by (Kole & Dey, 2012) through which they investigated the thermal conductivity and viscosity of surfactant free ZnO/ethylene glycol nanofluid, the viscosity of the nanofluid showed transition from Newtonian behavior at lower ZnO concentration to non-Newtonian characteristics at higher ZnO content and lower temperatures but

38

more importantly, the viscosity of the nanofluid was found to be nearly independent of ZnO nanoparticle loading. In addition, the large thermal conductivity enhancement and marginal viscosity penalty of the nanofluids were attributed to the superior fragmentation and uniform distribution of ZnO nanoparticle clusters in the base fluid. Through some research work to study the thermophysical properties of nanofluids especially the characterization of the viscosity of different nanofluids, it was observed that the measured viscosity is higher than the existing theoretical predictions (Maiga, et al., 2004; Nguyen, et al., 2007).

39

CHAPTER III

EXPERIMENTAL SETUP AND METHODOLOGY

An experimental rig was designed and built for the purpose of studying the thermal performance of the nanofluid through different duct geometry (see Figure 3.1). The validity of the result of an experiment is directly impacted by its construction and execution, which implies that attention to experimental setup and the method employed are very important. Therefore, it is pertinent to take time and effort to organize the experiment properly to ensure that the right type of data, and enough of it, is available to answer the questions of interest as clearly and efficiently as possible. Unfortunately, some authors have reported different results on the thermophysical and heat transfer parameters of nanofluids which is likely traceable to the method of obtaining the data. Therefore, it is very critical in order to minimize the measurement uncertainties and obtain accurate data.

This chapter discusses in detail, the experimental setup for obtaining the viscosity, pressure drop, thermal conductivity, viscosity and heat transfer measurements of silica nanofluids. The experimental setup, which comprises temperature control system, viscosity measurement system, thermal conductivity measurement system, the flow loop, calibration of instruments, determination of best experimental procedure and experimental uncertainties are discussed in detail.

3.1 Experimental Loop

The closed experimental loop comprises the mass flow meter, the gear pump, the reservoir, pressure transducers, the data acquisition unit, the thermocouples, the DC power supply unit and heat exchangers which are all connected using a ¼ inch stainless steel and flexible PVC tubing. The flexible tubing is incorporated in this experimental loop to accommodate different lengths of the test section. This flow loop can facilitate experiments for fluids flowing through tubes ranging from 6 mm to 500 μm I.D.
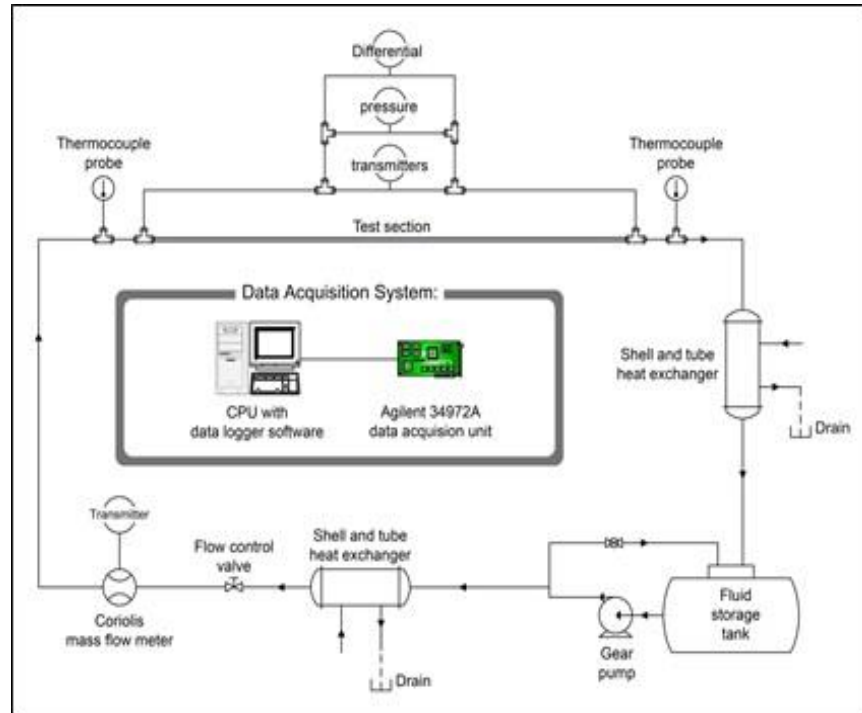

Figure 3.1 Schematic of flow loop for pressure drop and heat transfer measurements (Tiwari, 2012).

The reservoir houses the working fluid which were the NF and distilled water depending on the purpose of the experiment and the working fluid is circulated through the entire flow loop and then flow back to the reservoir. The gear pump provides the power for pumping the working

41

fluid to the entire flow loop and the counter-flow heat exchanger connected right after the gear pump removes the heat added during the fluid flow.

A second heat exchanger right after the test section removes any heat gained by the fluid when passing through the heated test section. The Coriolis mass flow meter measures the mass flow rate in the loop which is varied using a metering valve. Three pressure transducers are connected, one at the inlet and another at the outlet of the test section to measure the pressure drop with the other one for comparing the readings. These pressure transducers, connected for redundancy are expected to display the same readings under normal circumstances. The DC power supply unit supplies the current for heating up the test section during the heat transfer portion of the experiment. The thermocouples are cemented axially at equal distances along the test section for pressure drop and heat transfer analysis. The flow loop consisting of the pressure transducer, DC power supply and the mass flow meter are connected to the data acquisition unit (Agilent) for data gathering and further analysis.

3.1.1 The Reservoir

The reservoir is a cylindrical container made from PVC having a capacity of 15 liters and with diameter of 0.25m, length 0.3048m (see Figure 3.2) placed at about one meter above the gear pump in order to maintain the constant flow of the working fluid during the experiment. At the bottom of the reservoir a piping connects to the gear pump while at the top a bypass line and the line from the loop are connected.

Figure 3.2 Flow loop reservoir.

3.1.2 Gear Pump

A standard duty sealed gear pump shown in Figure 3.3, (model 35 F), manufactured by Liquiflo from stainless steel and which operates at variable speed with maximum rated speed of 1750 RPM and rated for a maximum flow of 13 LPM and maximum ΔP of 100 Psi was used for this experiment. Its suction side is connected to the reservoir and its discharge side is connected to a Tee dividing the flow through the closed loop and a bypass. It can support a minimum temperature of -40 degree Celsius, a maximum temperature of 260 degree Celsius and a maximum viscosity of 100,000 mPas. The gear pump has a wear plate which is a sacrificial part of the pump designed to protect the front and the rear housing from wear caused by continual contact with the sides of the gears.

43

Figure 3.3 The Liquiflow sealed gear pump

3.1.3 Mass Flow Meter

The mass flow meter shown in Figure 3.4 is a Micro Motion mass transmitter with an accuracy of ±0.05% of the flow rate connected to a 1700R model transmitter. The meter works based on the principle of the Coriolis Effect which is a deflection of moving objects when the motion is described relative to a rotating reference frame.

Figure 3.4 Micro Motion mass flow sensor connected to a 1700R model transmitter.

44

3.1.4 Pressure Transducers

Three Rosemount pressure transducers (model 3051) were used to measure different pressure gauges with an accuracy of +0.65% of span and connected to the inlet and outlet of the test section (see Figure 3.5). The first pressure transducers to the left captures the lowest pressure drops between 0 and 9 psi, the middle one is between 0 and 36 psi and the one to the far right measures between 0 and 300 psi. These pressure transducers are connected in parallel so that each of them captures the same pressure readings for a given flow rate but more importantly, they are connected in parallel so that a more accurate reading may be obtained. This arrangement is particularly useful to compensate for error in any of the transducers. The data acquisition unit is programmed to produce an alarm if a pressure drop reading is above the maximum for a given transducer after which a valve on the pressure transmitter isolates that particular transmitter.

Figure 3.5 Three Rosemount pressure transmitters (model 3051) connected in parallel.

3.1.5 Data Acquisition Unit

The data acquisition unit used for this experiment was manufactured by Agilent Technologies, Inc. (model 34972A) with a 20 channel multiplexer (see Figure 3.6). It measures

45

different input signals including temperature with thermocouples and is backward compatible with the USB 2.0 for easy connectivity to the PC. All thermocouples, mass flow meter, pressure transducer are attached to the channels of multiplexer for direct capture of measurements. The Agilent Benchlink Data Logger 3 is a free software used to control and program the channels, set the number of scans and capture data. The data acquisition unit is connected to the PC via a USB cable and the experiment was programmed to stop after 100 scans for each mass flow rate.

Figure 3.6 The Agilent data acquisition unit (model 34972A).

3.1.6 Thermocouples

One of the two thermocouples used for this experiment is a Neoflon PFA-insulated copper-constantan T-type quick disconnect thermocouple with miniature connector (see Figure 3.7). It is made from a 36 AWG thermocouple wire manufactured by Omega Engineering Inc. (model TT-T-36-SLE-1000). The tips of the two cables from the thermocouple was welded to form one thermocouple tip which are then cemented axially at equal intervals along the test section with the help of a high temperature and thermally conductive epoxy and catalyst from Omega (part no. 08-

46

101-16) . Special caution was taken to ensure that the tip was as small as possible so that measurement from each cemented point on the test section is very accurate. The thermally conductive epoxy was used to cement the thermocouples to the surface of the test section which also act as an electrical insulator, protecting the thermocouple and ensuring accurate temperature readings at specific points along the test section.
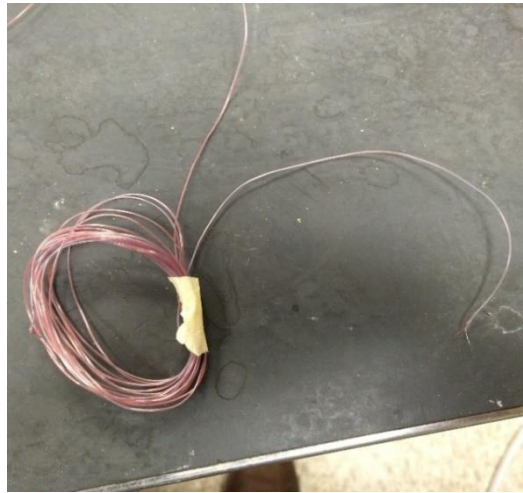

Figure 3.7 T-type thermocouple.

The second thermocouple, from Omega Engineering Inc. (model no. TMQSS-020U-6) is a copper-constantan 304 SS Sheath T-type quick disconnect thermocouple with miniature connector which are used for capturing the bulk fluid inlet and outlet temperatures at the entry and exit of the test section respectively. This thermocouple is 0.020 inches sheath diameter and 6 inches length and its welded tip is inserted into the middle of the flow path of the fluid with the help of a tee and a reducing compression fitting from Omega Engineering Inc. (part no. SSLK-116-18, 1/16*1/8). The thermocouple is then attached to the data acquisition unit where the bulk temperature is recorded.

3.1.7 DC Power Supply

The DC power supply is required for the heat transfer measurements in order to capture the temperature at each test points on the test section. The DC power supply is the N5761A from Agilent Technologies (see Figure 3.8), having a with single rated output of 6 V / 180A, 1080W and a measurement accuracy of ±300mA for current and ±6mV for voltage. The output from the DC power supply is connected to the test section through a copper strip silver soldered to the two ends of the test section using the epoxy. It also feature a remote load sensing control circuit that compensates for the voltage drop in the wires or improve load regulation.

Figure 3.8 N5761A Agilent DC power supply unit.

3.1.8 Test Section

For this research, four test sections of different geometries are investigated. The first and main test section is a rectangular brass C260 hollow bar, ASTM 135 of 3/32" in height, 3/16" in width, 0.014" in wall thickness and 12" in length (see Figure 3.11). The second test section is a square brass C260 hollow bar, ASTM 135 having 3/32" in height, 3/92" in width, 0.014" in wall thickness and 12" in length (see Figure 3.12), the third test section is a hexagonal brass C260

48

hollow bar having 3/32" in width across Flats, 0.014" in wall thickness and 12" in length (see Figure 3.13) and a circular brass C260 hollow bar, ASTM 135 having 1/8" in diameter, 0.014" in wall thickness and 12" in length .

The rectangular test section had ten thermocouples placed on its wider and smaller sides for capturing the temperature along the length of the test section. However, it is shown in Figures 3.9 and 3.10 that the placement of the thermocouples on either side of the test section had no significant effect on the measured temperatures.
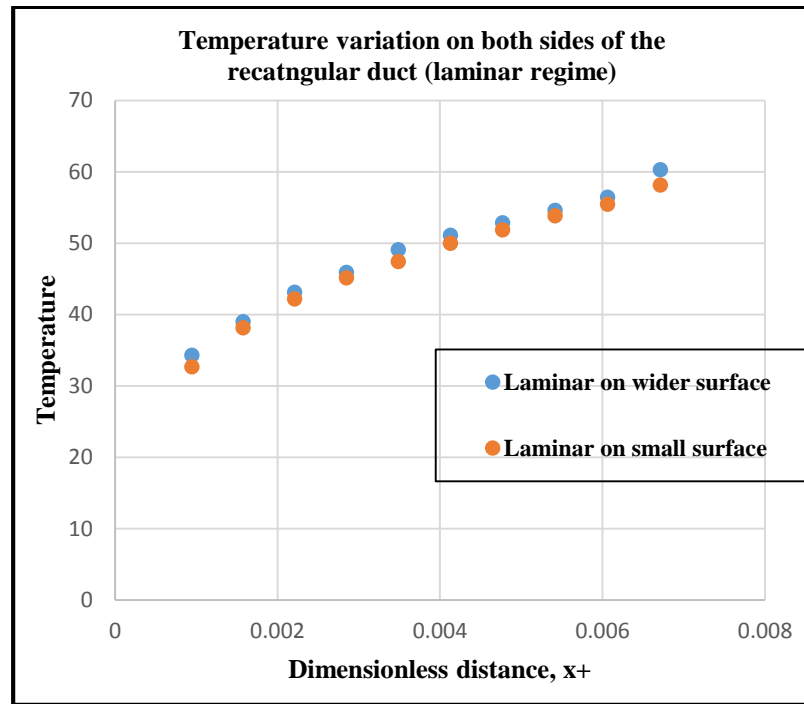

Figure 3.9 Plot of Temperature vs. Dimensionless distance x+ for rectangular test section (laminar regime).
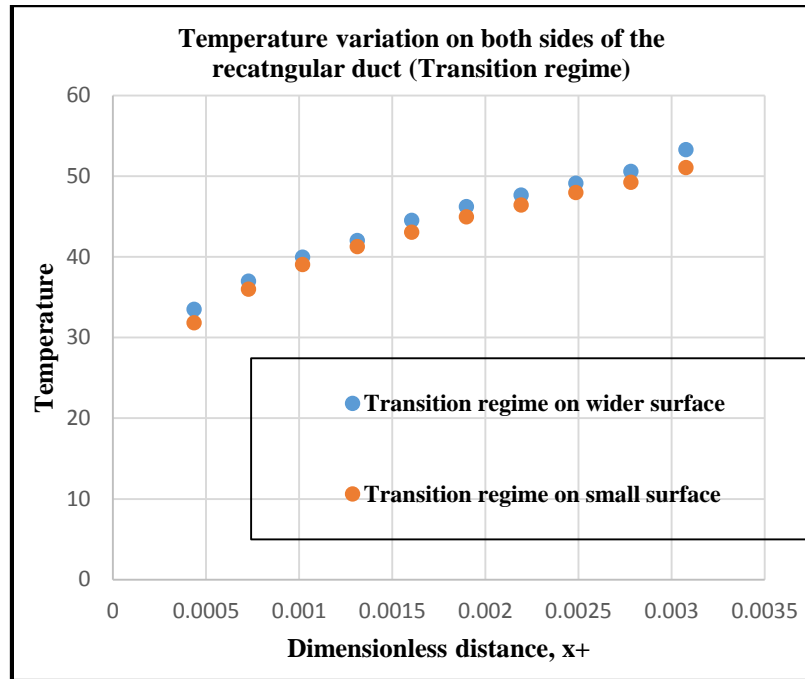
Figure 3.10 Plot of Temperature vs. Dimensionless distance x+ for rectangular test section (transition regime).

These test sections are connected to the flow loop with the help of graphite/polyimide ferrules of 40% graphite / 60% polyimide which help to seal and prevent leaks between the flow loop and the test section. These polyimide ferrules are able to support maximum operating temperature of 400°C because of their lower coefficient of expansion compared to other polyimide resins, thereby reducing the tendency of the nuts loosening during the heated experiment.

Figure 3.11 Rectangular test section with thermocouples tips cemented axially along the surface and two copper strips at the end for supplying DC power.

Figure 3.12 Square test section with thermocouples tips cemented axially along the surface using Omega bond cement.

Figure 3.13 Hexagonal test section with thermocouples tips cemented axially along the surface and two copper strips at the end for supplying DC power.

3.1.9 Heat Exchangers

For this experiment, two counterflow heat exchangers were used to regulate the heat. They were fitted coaxially to the ¼ inch tubing in the flow loop at the entry and exit. The purpose of the heat exchanger placed just after the gear pump is to eliminate the heat added from the pump and maintain a steady inlet temperature to the test section and the second heat exchanger was placed after the test section to remove the heat added during heating of the test section for the heat transfer experiments. These heat exchangers are each ½ inch diameter stainless steel tubing with length of 38 inches; fitted with the help of a ½ inch Tee connection and a Swagelok tube fitting on both ends. The Swagelok tube fitting possesses a ½ inch thread connected to the Tee at one end and a ¼ inch compression fitting at the other end which maintains a seal between the ½ inch tubing and the ¼ inch tubing while the other free end of the tube is connected to a cold water supply by a ½ inch PVC tubing.

3.2 Experimental Procedure

The following are the actions taken in an attempt to investigate the behavior and characteristics of nanofluids as they flow through small diameter tubes. Two major measurements are made: pressure drop and heat transfer measurements.

3.2.1 Pressure Drop Measurement

1. Begin by starting the data acquisition unit, the pressure transducers, the gear pump, the mass flow meter and the Agilent software on the PC.

2. Adjust the speed of the pump to match the desired mass flow rate and use the metering valve to get the actual flow rate while ensuring that the bypass valve is open to limit the strain on the pump.

3. Open the reservoir for fluid flow and open the cold water tab to supply the heat exchangers Observe the pressure transducers for stability since the pressure transducers should indicate very close readings.

4. Allow about 5 minutes for the system to reach steady state and then take the first data set to obtain the minimum and maximum values of the mass flow rate for the entire experiment.

5. Increase the speed of the gear pump and fine tune again using the metering valve until the next desired mass flow rate is achieved. Allow 5 minutes for stability and then take the readings. These readings are exported to the Microsoft Excel format via the Agilent software for further analysis.

6. Continue to increase the speed of the pump to get the next mass flow rate and stop when the maximum flow rate is reached. Continue to observe unexpected performance from the devices or readings to detect errors at an early stage.

3.2.2 Heat Transfer Measurements

1. The heat transfer measurement is completed concurrently with the pressure measurements in order to save time and take readings at the same set of flow rates. For this purpose, a fiber glass insulation (R-25) was used to properly insulate the test section at the beginning of the experiment.

3. After the initial pressure drop measurement is recorded, proceed by turning on the DC power supply. Ensure that the bypass valve is open and keep the cold tap water running to supply the heat exchanger. This is the time to record the corresponding heat transfer measurement for that particular mass flow rate.

4. Allow about 10 minutes for the system to reach a steady state after which the data can be recorded and exported to Microsoft Excel for further analysis. It is important to observe the data captured for unexpected errors and to verify a steady state.

5. Return the DC power supply back to zero readings to allow the test sections to cool down for the next pressure measurements while maintaining the cold water supply to the exchanger.

5. After the first reading, subsequent heat transfer measurements are recorded concurrently with the pressure measurements. The only difference between these two measurements is the fact that the DC power supply is turned on during the heat transfer measurement for the purpose of heating the test section. It is returned to zero readings after the readings are captured.

6. The process is repeated until maximum flow rate has been achieved. The bulk fluid temperature difference between the inlet and the outlet should not be less than 2.5°C, otherwise halt the experiment.

54

7. Always ensure that the DC power supply is turned off first and then the pump because stopping the pump first while heating the test section will create excessive heat in the test section with no fluid flowing. This might damage the test section and even the thermocouples. For nanofluid, excessive heat can cause dry out and clog up the test section.

3.3 Experimental Uncertainties

3.3.1 Friction Factor

The friction factor is given by the Darcy-Weisbach equation which is expressed mathematically as:

$$f = \frac{2 \Delta P D_h}{\rho L V^2} \tag{3.1}$$

The velocity term in this relation is computed as:

$$V = \frac{m}{\rho A_i} \tag{3.2}$$

The flow area (rectangular test section) is given as:

$$A = wl \tag{3.3}$$

Therefore, the velocity can be written as:

$$V = \frac{m}{\rho wl} \tag{3.4}$$

Finally, the friction factor can be written as:

$$f = \frac{2 \Delta P D_h \rho w^2 L}{m^2} \tag{3.5}$$

Hence, the Equation (3.5) above shows that the friction factor depends upon 1) pressure drop, 2) inside diameter of the test section, 3) density of the fluid flowing through the test section, 4) length and width of the test section, and 5) mass flow rate of the fluid. The uncertainty inherent in determining the pressure drop, mass flow rate and the length of the test section can be controlled depending on the accuracy of the procedure employed for data gathering. However, the uncertainty in certain parameters such as test section internal diameter depends on the product's accuracy from the manufacturer and the accuracy of the pressure transmitter is already specified as +0.65% of span from the manufacturer.

While taking readings, careful attention was given so that the process reached steady state and all of the three transducers were reading the same pressure drop. However, when taking readings with water at low Reynolds number and higher tube diameter, the uncertainty in the measurement of pressure drop seemed to be high which were indicated by slightly different reading of the three pressure transmitters. The situation seemed better when using nanofluid as the working fluid. In this case the readings from the lower range pressure transmitter were used for data analysis.

The uncertainty in the inside diameter of the test section is a major factor that affects the measurement of friction factor. From Equation 3.5 it is clear that the friction factor relates to the fifth power of the inside diameter. The tolerance provided by the manufacturer is 0.002 inches. The accuracy of the mass flow meter is specified as ±0.05% of the flow rate. Here also extra attention was given to capture a steady state process. The uncertainty of the tube length is determined by the accuracy of the measurement scale used for measuring the tube. The least count of the measurement scale used is ± 0.25 inches. Repeated measurements were taken to avoid any error. The uncertainty for the length of the tube is given as ± 0.25 inches. The operating range of

56

the experiment was from 5°C till 60°C. It is assumed that the particle density stays constant over this range whereas the density of water may change slightly.

3.3.2 Heat Transfer

The heat transfer is quantified in terms of the Nusselt number. The Nusselt number is given as:

$$Nu = \frac{hD_i}{k}$$ (3.6)

The convective heat transfer coefficient is calculated from the following equation

$$h = \frac{q}{T_{wi} - T_b}$$ (3.7)

$$q = \frac{dQ}{\pi D_i dx}$$ (3.8)

The inside wall temperature T$_{wi}$ is calculated from the outer wall temperature T_{wi} by using the conduction equation given as:

$$T_{wi} = T_{wo} - \frac{qD_i x}{2k_s L} ln \frac{D_o}{D_i}$$ (3.9)

The bulk fluid temperature is assumed to vary linearly from the inlet of the test section to the outlet and for any axial distance along the test section, it is given as

$$T_{b,x} = T_{b,in} + \frac{x}{L}(T_{b,out} - T_{b,in})$$ (3.10)

3.4 Calibration of Instruments

3.4.1 Thermocouple Calibration

The accuracy of result for the heat transfer measurements are influenced by the temperature measurements which are captured by the thermocouples. This implies that all the thermocouples used in this experiment must be calibrated to validate their accuracy. Both types of thermocouples were calibrated using the temperature bath and an RTD. The temperature range for calibration was from around 7–70°C, which falls under the operating temperature range for this experiment. It can be seen from Figures that the thermocouple readings are in close agreement with the RTD readings in the temperature range of 7–70°C. The maximum difference between the calibrated thermocouples and the RTD is 0.31°C.

3.4.2 Viscometer Calibration

The Brookfield viscometer was calibrated from the manufacturer but its accuracy needs to be validated for the experiment and a standard calibration fluid with a viscosity of 493 cP at 25°C was used for that purpose. The same procedure for measuring fluid viscosity was followed using the enhanced UL adapter. The results of the calibration for the standard viscosity fluid are shown in Figure 3. From the figure, it can be inferred from the heating curve that the viscosity at 25°C was 493.09 cP and for the cooling curve, the viscosity at 25°C was 494.39 cP. These values lie within the uncertainty of the instrument (±2 cP) and it implies that the procedure for taking the viscosity measurements was accurate.

3.4.3 Pressure Transmitters Calibration

المنارة للاستشارات

www.manaraa.com

In order to calibrate the three pressure transducers, a pneumatic hand pump from Ametek (model T-970, range 0 to 580 psi), shown in figure 3.18 and digital electronic gages from Dwyer (model DPG-107, range 0–300 psi, and model DPG-104, range 0–50 psi). By exerting pressure definite amount of pressure from the hand pump, the output voltage from the transducers was recorded. This measurement was used to calibrate the pressure transducers according to the following procedures:

1. Connect the digital pressure gauge to the hand pump. Then connect the hand pump to the high pressure side of the pressure transmitter.

2. Apply certain amount of pressure by pumping the hand pump. Leave the system for about 2 minutes. If the pressure has reduced, check the connections for leak using soap solution.

3. Apply certain amount of pressure and record the voltage corresponding to the pressure.

4. Increase the applied pressure by 5 psi and record the voltage. Repeat this step until the higher range of the pressure transmitter has been reached.

5. Repeat the same steps for other two pressure transmitters.

CHAPTER IV

RESULTS AND DISCUSSIONS

This chapter focuses on the presentation and discussion of the experimental findings. The experimental data for the four test sections of different geometries was analyzed and compared with relevant correlations. The main working fluid for the experiment was a 9.58% by volume fraction of SiO_2/water nanofluid containing nanoparticles of an average size of 20 nm. The thermophysical properties of water and the SiO_2/water nanofluid, that is; the viscosity and thermal conductivity; measured by (Sharif, 2015) was used to analyze the experimental data from the experiment. For the validation of the experimental methodology, distilled water was passed through the flow loop and the result was compared with existing data from literature.

4.1 Validation of the Experimental Procedure Using Distilled Water

Working from theory, it was necessary to ascertain if the experimental methodology was correct and suitable for generating the experimental result and to validate the accuracy of the instruments. This was achieved by passing distilled water through the flow loop before passing the main working fluid (SiO_2/water nanofluid) through it with the intention of matching the available data for distilled water. This validation was necessary to ascertain the accuracy and reliability of the experimental system for capturing the rheological behavior of the main fluid which is nanofluid. In addition, water was used for the validation because there are well established data

60

for water in the literature and based on the fact that repeatability of these data within a certain allowable margin of error validates the correctness of the methodology.

4.2 Thermophysical properties of Distilled Water

As stated earlier, the viscosity and thermal conductivity data for distilled water measured by (Sharif, 2015) was validated in this work in comparison with existing data from literature. These thermophysical properties are only needed for the analysis of the experimental data for this thesis but it is not the focus of this work.

4.2.1 Thermal Conductivity Result of Distilled Water

Amongst all the thermophysical properties studied, thermal conductivity has been identified as the main property responsible for the enhancement observed in nanofluids. The standard values of the thermal conductivity of distilled water within the temperature range of 1^oC to 45^oC was extracted from literature (Ramires, et al., 1994). It was then compared with the experimental data. Figure 4.1 shows the plot that compares the experimental and standard thermal conductivity vs. temperature for distilled water.
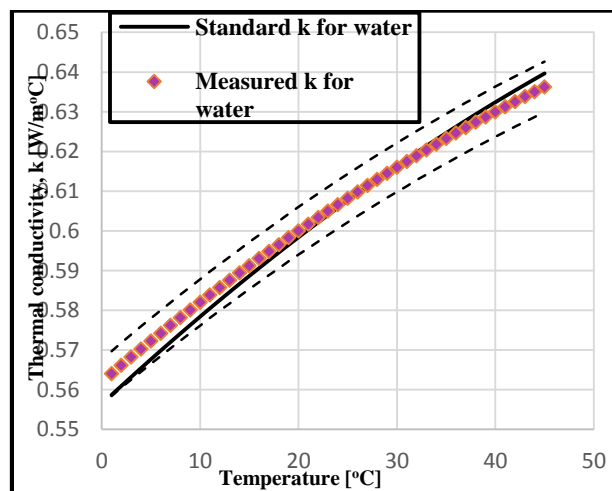
Figure 4.1 Comparison between experimental and standard values of thermal conductivity of distilled water.

61

It can be observed that the experimental value of the thermal conductivity of water matches that of the standard values available in literature with ±1% margin of error. As a result of the observed agreement between the experimental and standard values of the thermal conductivity, it can be inferred that the methodology is suitable for thermal conductivity measurement and appropriate for nanofluid which is the main working fluid under investigation. As expected, the experimental thermal conductivity of water increases with increasing temperature for temperature range of 0°C to 45°C.

4.2.2 Friction Factor Results of Distilled Water

Again, in order to demonstrate the validity and accuracy of the methodology for measuring the friction factor of the nanofluid, just like a model should be verified if it were a numerical investigation, the Darcy-Weisbach equation shown in Equation 4.1, valid for laminar flow was used to calculate the friction factor of water using the experimental data. This equation, valid for estimating the friction factor of Newtonian fluids is expressed as:

$$f = \frac{2\Delta P D_h}{\rho L V^2} \tag{4.1}$$

But, recall that, $$f_f = \frac{f}{4} \tag{4.2}$$

Consequently, $$f_f = \frac{\Delta P D_h}{2\rho L V^2} \tag{4.3}$$

The calculated experimental friction factor was then compared with existing theoretical relation valid for single phase Newtonian fluids such as distilled water. In fluid mechanics, it has been established that the fanning friction factor for water flowing through circular, smooth ducts is shown in Equation (4.4) below (White, 2008):

62

$$f_f = \frac{16}{Re} \tag{4.4}$$

However, the values of the friction factors for other noncircular ducts which are also investigated in this work are stated for rectangular, hexagonal and square ducts in Equations (4.5), (4.6) and (4.7) respectively (Cengel, 2007).

$$f_f = \frac{15.55}{Re} \tag{4.5}$$

$$f_f = \frac{15.05}{Re} \tag{4.6}$$

$$f_f = \frac{14.23}{Re} \tag{4.7}$$

The Darcy-Weisbach relation shown in Equation (4.3) above clearly shows that fanning friction factor is a function of pressure drop, the hydraulic diameter of the test section, the density of the fluid, the length of the test section and the velocity of the fluid which are experimentally determined. Throughout this analysis, the Equation (4.3) was used to estimate the experimental fanning friction factor which is ¼ of the Darcy friction factor as shown in Equation (4.2). These calculated experimental fanning friction factors were plotted against Reynolds number for the four duct geometries which are rectangular, square, circular and hexagonal geometries in the laminar regime and compared with relevant correlations. The plot is compared with the values calculated from Equation (4.8) given by Morrison (2013) correlation valid for all Reynolds number (laminar, transitional, and turbulent) as shown in Figure 4.2. Owing to the fact that the four test sections have very close hydraulic diameters and equal length of 12 inches, the hydraulic diameter was used as a basis for their comparison. The hydraulic diameters of the rectangular test section is 0.093 inch while that of the hexagonal, circular and square test sections is 0.097 inch.

63

$$f = \left[\frac{0.0076\left(\frac{3170}{Re}\right)^{0.165}}{1+\left(\frac{3170}{Re}\right)^{7.0}}\right] + \frac{16}{Re} \qquad (4.8)$$

From the plot shown in Figure 4.2, it is evident that the experimental values of friction factor of all the ducts lie within ±20% of what was predicted by the Morrison (2013) correlations for the laminar regime. This observation validates the methodology and the reliability of the experimental rig for measuring friction factor and was subsequently used or the measurement of the friction factor of the silica/water nanofluid.
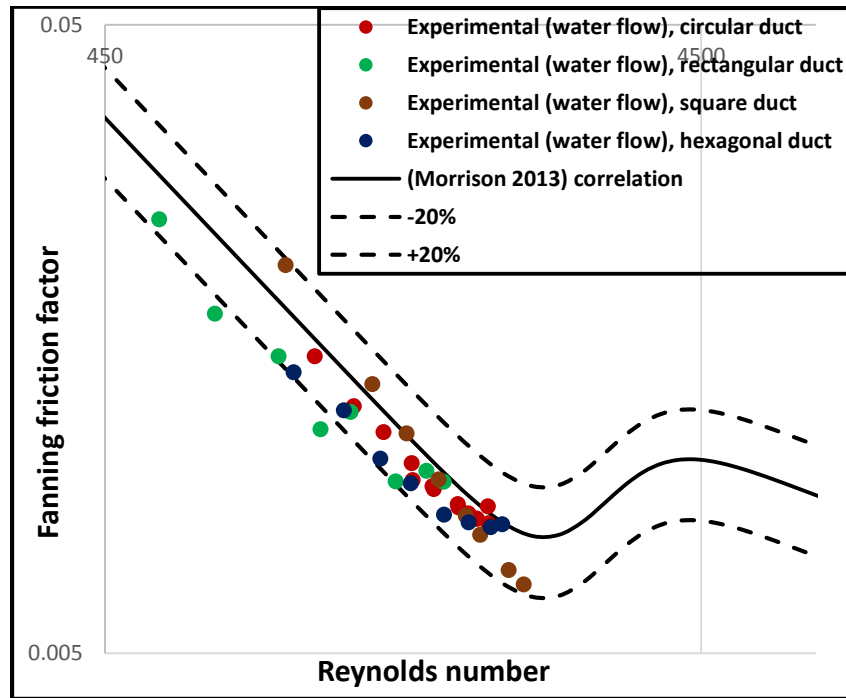
Figure 4.2 Plot between the experimental fanning friction factors of water in different test sections vs. Reynolds number compared with Morrison (2013) correlations.

In addition, the Figures 4.3-4.6 below show the direct comparison of the experimental values of the fanning friction factor for water in the laminar regime with the corresponding theoretical friction factor correlations for water in the laminar regime, given by Equations (4.4), (4.5), (4.6), (4.7) above for the circular, rectangular, hexagonal and square ducts respectively. For the hexagonal and square ducts, the theoretical relation has predicted the experimental result within

64

±15% error. The theoretical relation predicted the experimental fanning friction factors for the circular and the rectangular duct with ±10% and ±20% respectively. This observation validates the experimental setup and methodology for pressure drop and friction factor measurements and will consequently be extended to the nanofluid.

Also, it was observed that transition occurs at different Reynolds number as shown by the deviation in flow pattern in the Figures 4.3-4.6 below. To be more precise, transition occurs in the square, hexagonal, circular, and rectangular ducts at Reynolds numbers of approximately 2260, 2000, 1900 and 2200 respectively. This observations showed that the duct geometry affect when transition occurs in fluids. The point where transition occurs depend on the smoothness of the entrance but for this research, the smooth was assumed to be smooth.
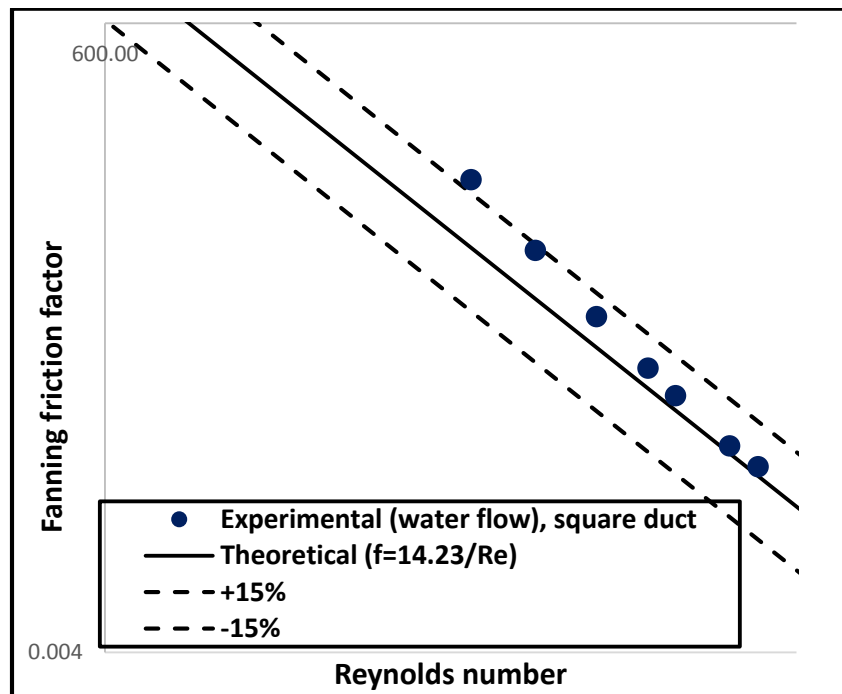
Figure 4.3 Comparison of the experimental friction factor and theoretical friction factor vs. Reynolds number for water in square duct.

65
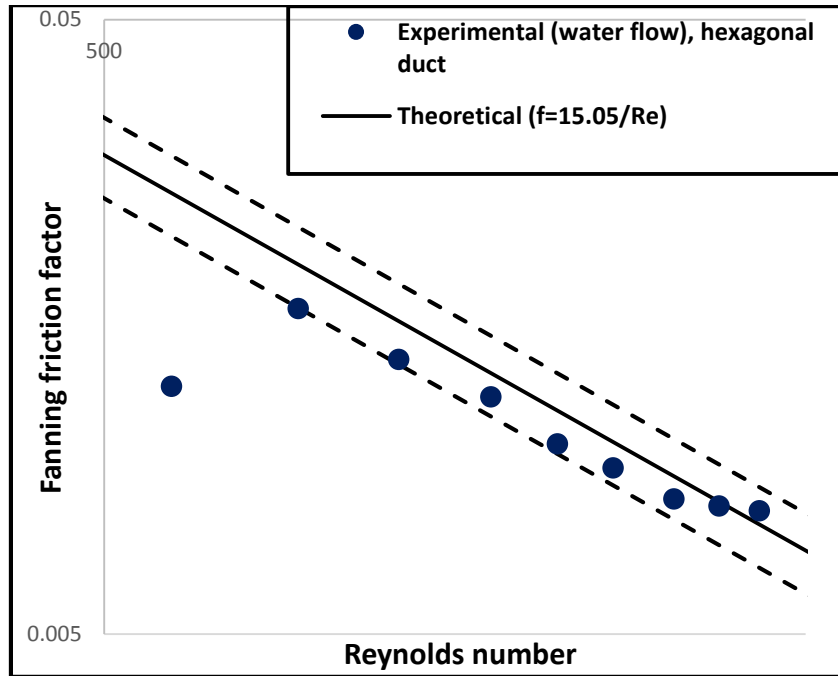
Figure 4.4 Comparison of the experimental friction factor and theoretical friction factor vs. Reynolds number for water in hexagonal duct.
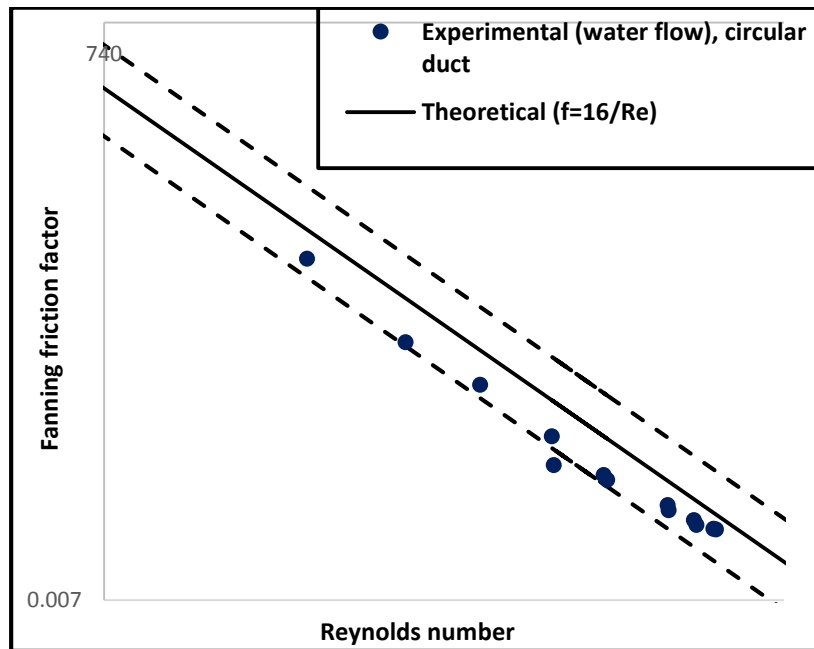
Figure 4.5 Comparison of the experimental fanning friction factor and theoretical friction factor vs. the Reynolds number for water flowing in the circular duct.
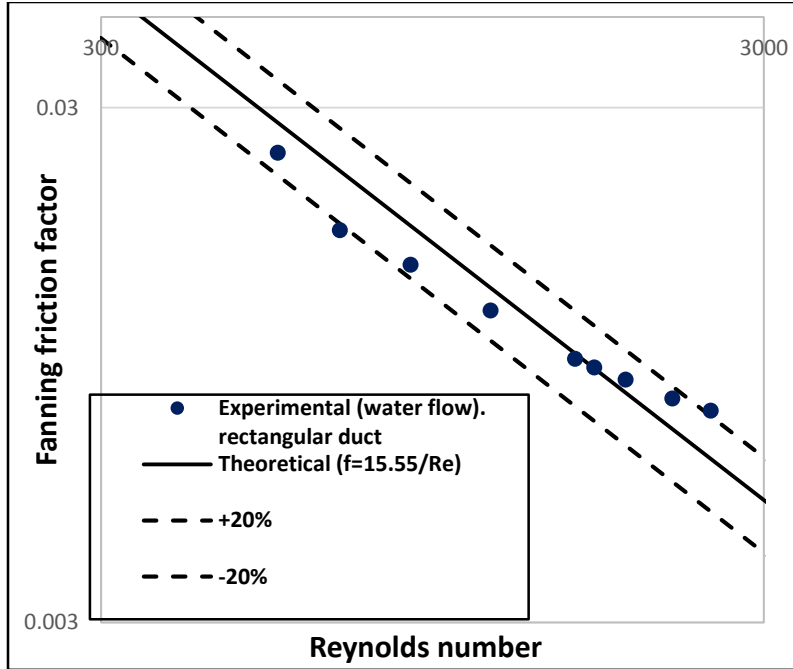
66

Figure 4.6 Comparison of the experimental friction factor and theoretical friction factor vs. Reynolds number for water in rectangular duct (aspect ratio 2:1).

4.2.3 Heat Transfer Results of Distilled Water

Similarly, before conducting heat transfer measurements on the nanofluid, the reliability and accuracy of the experimental system was tested using distilled water as the working fluid before passing the nanofluid through the flow loop. Heat is often characterized in terms of Nusselt number which is a ratio of the convective to conductive heat transfer across normal to the boundary. The Nusselt number is expressed as a function of the heat transfer coefficient as follows:

$$Nu = \frac{hD_h}{k} \tag{4.9}$$

In Equation (4.9), the convective heat transfer coefficient, h is calculated as follows:

$$h = \frac{q}{T_{wi} - T_b} \tag{4.10}$$

From Equation (4.15), q is the heat flux per unit area, expressed as:

67

$$q = \frac{1}{P}\frac{dQ}{dx}$$
(4.11)

From the Equation (4.11), P represents the flow perimeter and x is the axial distance along the heated test section.

$$Q = I*V$$
(4.12)

The inside wall temperature (T_{wi}) is calculated from the outside wall temperature (T_{wo}) by using the conduction equation given as:

$$T_{wi} = T_{wo} - \frac{qD_h x}{2k_s L}\ln\frac{D_o}{D_i}$$
(4.13)

Where L is the length, D_h is the hydraulic diameter of the test section, and k_s is the thermal conductivity of the wall. The bulk fluid temperature is assumed to vary linearly from the inlet of the test section to the outlet and for any axial distance along the test section, it is given as

$$T_{b,x} = T_{b,in} + \frac{x}{L}(T_{b,out} - T_{b,in})$$
(4.14)

Where $T_{b,in}$ the inlet fluid is bulk temperature [°C] and $T_{b,out}$ is the outlet fluid bulk temperature [°C]. The experimental results were recorded at a constant heat flux of 200W/m^2 and the Reynolds number were in the range 500≤Re≤6500. Consequently, the experimental results was compared with the Nusselt number predictions given by the (Lienhard & Lienhard, 2015) correlation applicable for the laminar regime under constant heat flux boundary condition as given by Equations (4.15) and (4.16) respectively. The average experimental Nusselt numbers were calculated from the local Nusselt number using Equation (4.14) and the theoretical Nusselt numbers were calculated using thermophysical properties at the average fluid temperature between inlet and outlet of the test section. The (Lienhard & Lienhard, 2015) correlation describes the Nusselt number for a thermally developing flow, expressed mathematically as:

68

$$Nu = 4.364 + 0.263 \, (\tfrac{x^+}{2})^{-0.506} \exp[\left(-41\tfrac{x^+}{2}\right)] \qquad (4.15)$$

From Equation (4.20), x+ is the dimensionless distance given by:

$$x^+ = \frac{2x}{D_i Re Pr} \qquad (4.16)$$

Figure 4.7 below show the plot between the experimental Nusselt number and the Reynolds number for the four duct geometries, from which it can be inferred that Nusselt number increases with increasing Reynolds numbers. However, the rectangular duct were observed to have the highest and approximate Nusselt number followed by the circular duct while the square duct showed the lowest Nusselt number. This observation was observed throughout the entire flow.
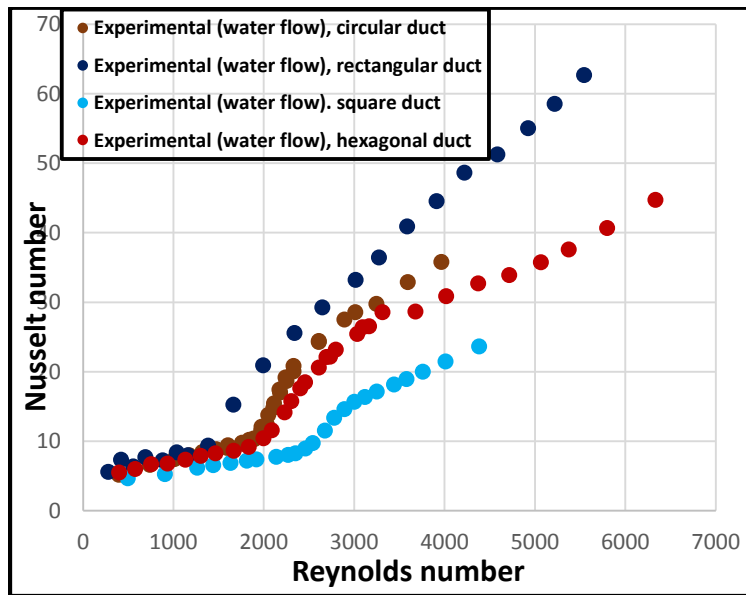
Figure 4.7 Experimental Nusselt number vs. Reynolds number for distilled water flowing through different duct geometries.

In addition, the experimental values of Nusselt number was compared with the (Lienhard & Lienhard, 2015) as shown in Figures 4.8 to 4.11. It is evident that the measured values lie within ±15% to ±20% of what was predicted by the Lienhard and Lienhard (2015) correlation for all the

duct geometries. Therefore, going by the fact that Nusselt number are in agreement with these correlations for all the duct geometries, the experimental procedure is validated and experiments for heat transfer measurements of the nanofluid was performed.
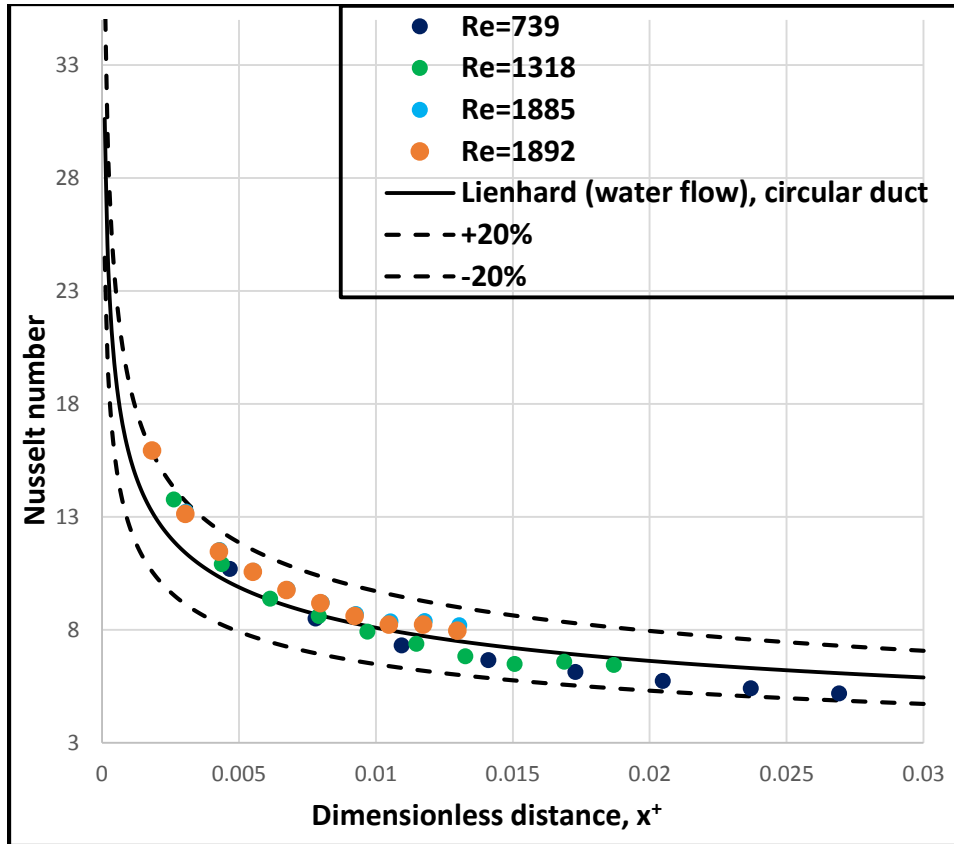

Figure 4.8 Plot showing the experimental Nusselt number vs. dimensionless distance given by the Lienhard & Lienhard (2012) correlation for water flowing through the circular duct.
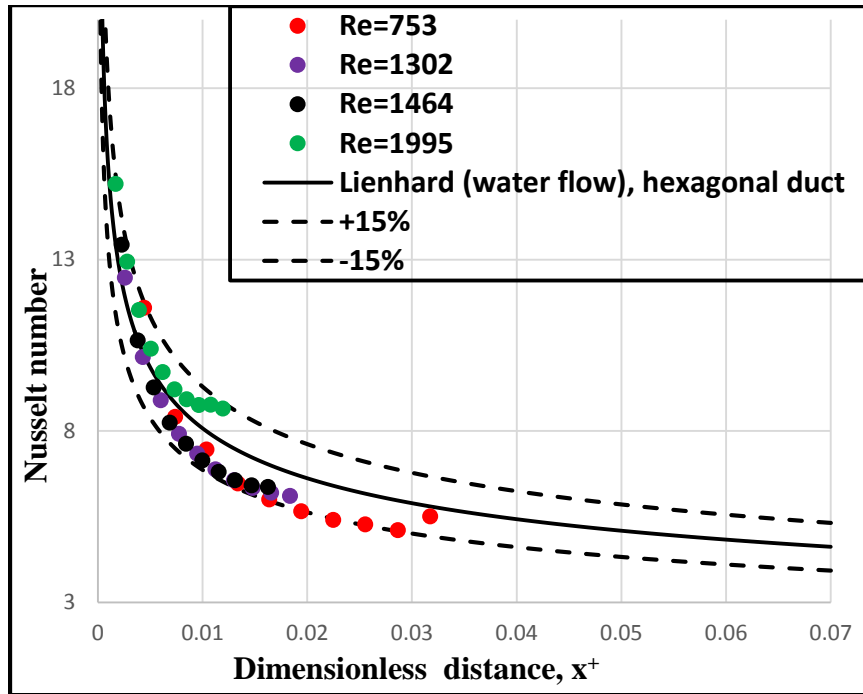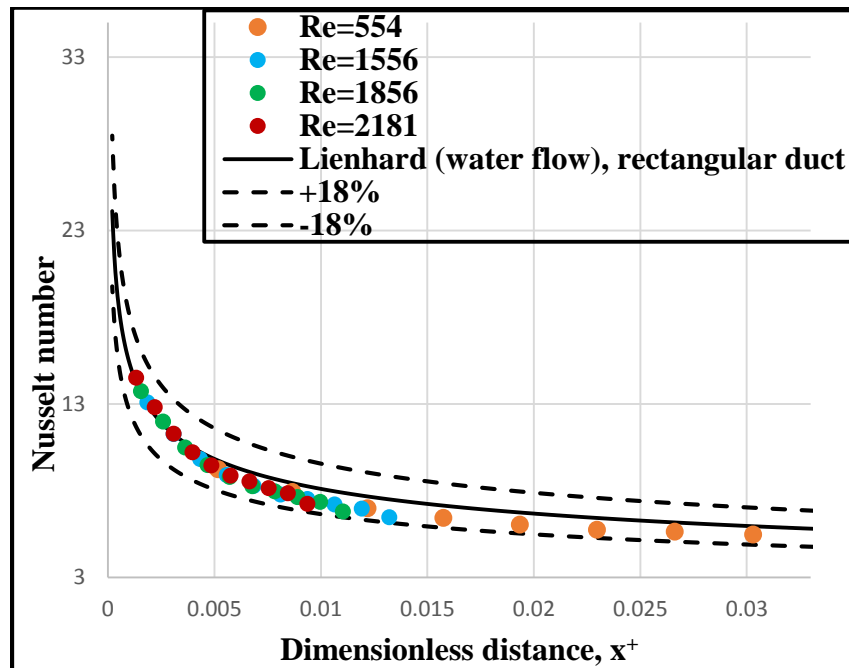
70

Figure 4.9 Plot showing the measured Nusselt number vs. dimensionless distance given by the Lienhard & Lienhard (2012) correlation for water flowing through the hexagonal duct.

Figure 4.10 Plot showing the measured Nusselt number vs. dimensionless distance given by the Lienhard & Lienhard (2012) correlation for water flowing through the rectangular duct.
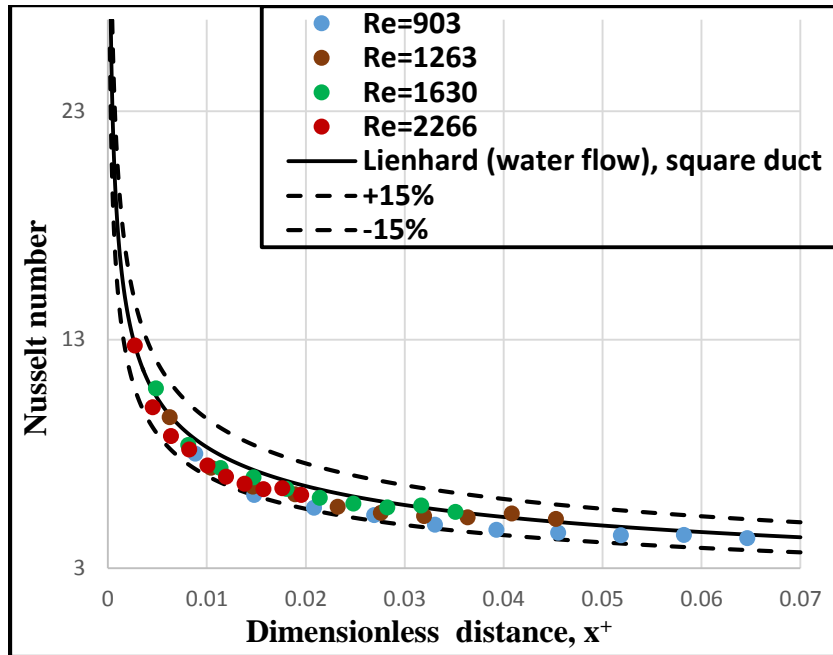
71

Figure 4.11 Plot showing the measured Nusselt number vs. dimensionless distance given by the Lienhard & Lienhard (2012) correlation for water flowing through the square duct.

4.3 Thermophysical properties of the Nanofluid

After the validation of the experimental procedure using distilled water, the experiment was repeated for the nanofluid following the same procedure and methodology.

4.3.1 Thermal conductivity of Nanofluids

The thermal conductivity measurements for the NF was performed by Sharif (2015) for temperature range of 1°C to 50°C and the available data for the NF was used in the analysis of this experimental data. The Figure 4.12 below represents the plot of the thermal conductivity of the NF and water vs. temperature from which it was observed that the thermal conductivity of the NF was higher than that of water but the thermal conductivity of the NF measured from 1°C to 50°C did not increase as much as that of the water. The observed increase in the thermal conductivity of the NF can be attributed to the higher thermal conductivity of the nanoparticles dispersed in the water.
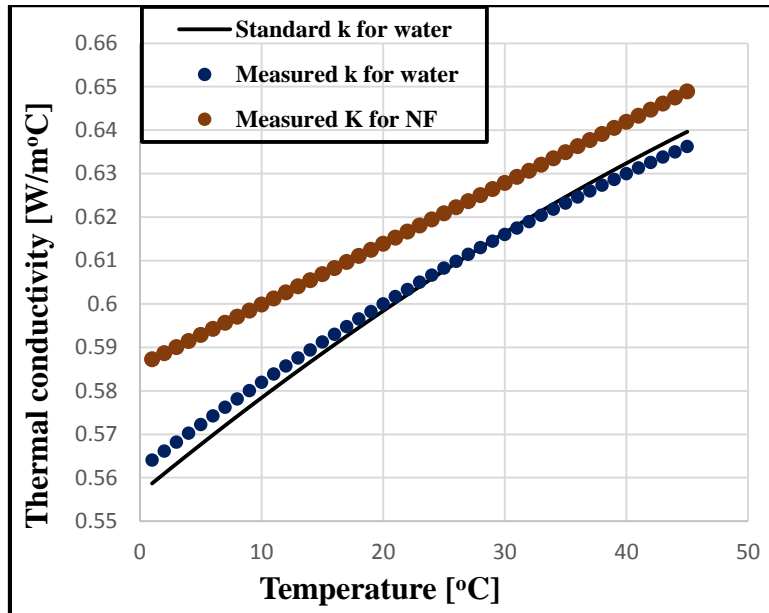
72

Figure 4.12 Comparison of the thermal conductivity vs. temperature for water and NF.

The thermal conductivity of the nanofluid was observed to be greater than that of water by 9.88% for the temperature range of 7°C to 50°C and the thermal conductivity of water increased by 11.1% within the same temperature range. The thermal conductivity of both the nanofluid and water was observed to increase with temperature over the entire temperature range and the thermal conductivity of the nanofluid is higher than that of water at all temperature points. Therefore, it has been established that the nanofluid has a better thermal conductivity compared to the base fluid.

4.3.2 Viscosity of the NF and its non-Newtonian behavior

In the field of rheology of fluids, fluids are classified as Newtonian and non-Newtonian based on their viscosities which is the fluid's tendency to resist gradual deformation by shear or tensile stress. For Newtonian fluids, the relationship between the shear stress and the shear rate is linear passing through the origin whose constant of proportionality is the coefficient of viscosity.

73

On the other hand, for non-Newtonian fluids, the relationship between the shear stress and the shear rate is different and non-linear. Non-Newtonian fluids have been classified as pseudoplastic, dilatant, plastic, thixotropic and rheopectic fluid engineers working in the field of rheology. The classification of a fluid to the Newtonian and the non-Newtonian categories have been adjudged to extremely depend on the experimental conditions under which the measurements were made (Metzner & Reed, 1955). The relation of shear rate and shear stress is given for Newtonian fluid as follows:

$$\tau = \mu \frac{du}{dy} \tag{4.17}$$

From Equation (4.17), τ= shear stress, $\frac{du}{dy}$= rate of shear and μ= constant of proportionality, known as viscosity. Any fluid not following the above relation is called a non-Newtonian fluid. The plot of the shear stress vs. the shear rate measured at 45℃ is shown in Figure 4.13, from which it can be observed that the slope is not linear. The shear stress was observed to increase with increasing shear rate and this type of behavior is exhibited by only shear thickening non-Newtonian fluid. Therefore, the silica/water nanofluid is a dilatant non-Newtonian fluid. For this type of non-Newtonian fluids, the slope of the plot is called apparent viscosity and this viscosity increases with shear rate. The viscosity also increases with increasing particle concentration.
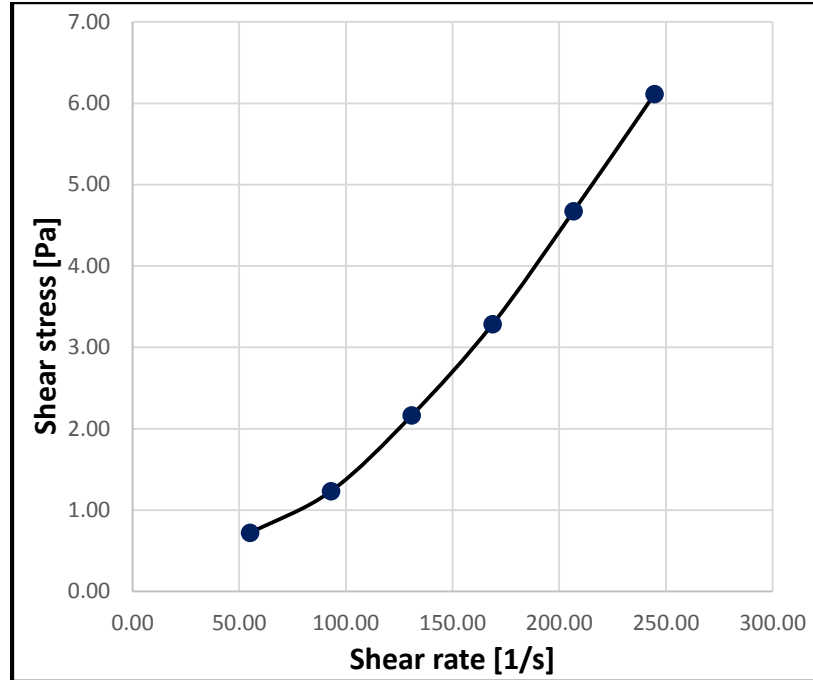
Figure 4.13 Plot of the shear stress vs. shear rate of the NF measured at 45°C.

Consequently, in order to determine the apparent viscosity of the NF as it varies with temperature, the power law model was used. The power law model is widely used for relating the wall shear stress and the shear rate of non-Newtonian fluids for a pressure driven pipe flow as follows:

$$\tau_w = \frac{D\Delta P}{4L} = K' \left(\frac{8V}{D}\right)^{n'} \tag{4.18}$$

In Equation, (4.18), n' (the flow behavior index is the physical property of the fluid which characterizes its degree of non-Newtonian behavior.) and K'(the consistency index) are the slope of the graph and intersect, obtained from the logarithmic plot of shear stress and shear rate respectively (Metzner & Reed, 1955). The greater the divergence of n' from unity, the more non-Newtonian is the fluid. For this experiment, the fluid n' was range from 1.08 to 1.34 for the

different duct geometries and the fluid can be said to be a dilatant non-Newtonian fluid because the value of n' is greater than unity.

4.4 Friction Factor Results of the Nanofluid

An attempt to investigate the change in the experimental friction factors of the NF and the base fluid (water) in each duct geometry led to the plot shown in Figures 4.14 to 4.17 for the circular, rectangular, hexagonal, and square ducts respectively. In the same vein, there was no significant change in the experimental friction factors between the NF and water. It was however observed that the NF reached transition earlier compared to the water and this could be traced to the migration of the particles to the boundary layer causing eddies.

Interestingly, the theoretical friction factor correlation developed for single phase fluids in the laminar regime as given in Equations (4.4) to (4.7) has successfully predicted the experimental data for the NF within ±25%. This somewhat greater deviation could be attributed to the presence of the nanoparticles and the inherent problems associated with colloidal suspensions such as sedimentation. These plots are shown in Figures 4.18 to 4.21 below.

The friction factors for the NF are measured for the four test sections whose geometry are rectangular, hexagonal, circular and square; having an equal length of 12 inches and very close comparable hydraulic diameters. The effect of the duct geometry on the experimental values of the friction factors in the laminar regime was investigated through the plot of the estimated friction factor of each duct vs. the estimated Reynolds number for the NF flow (see Figure 4.22). From this graph, it was observed that all the ducts were overlapping and the effect of the duct geometry on the friction factor was not significant.

76

On the other hand, Figure 4.23 shows the plot comparing the experimental pressure drops in both the NF and water against the mass flow for the rectangular, hexagonal, circular and square ducts. From the graph, there was no significant difference in pressure drops for each duct for the water and NF flow, but it was evident that the pressure drop in the circular duct was slightly higher the other ducts. Also, the pressure drops of the NF and water increased with increasing Reynolds number. Therefore, the circular duct exhibited the highest pressure drop which is consistent with reported results from existing literature.
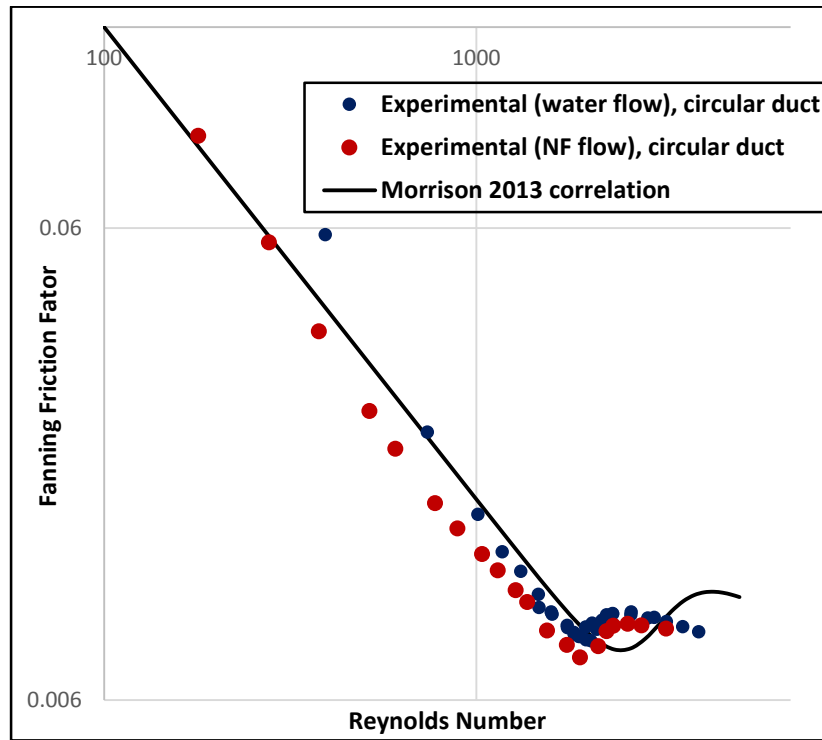
Figure 4.14 Comparison of the experimental friction factor with theoretical friction factor correlation vs. Reynolds number for water and NF flowing through the circular duct.
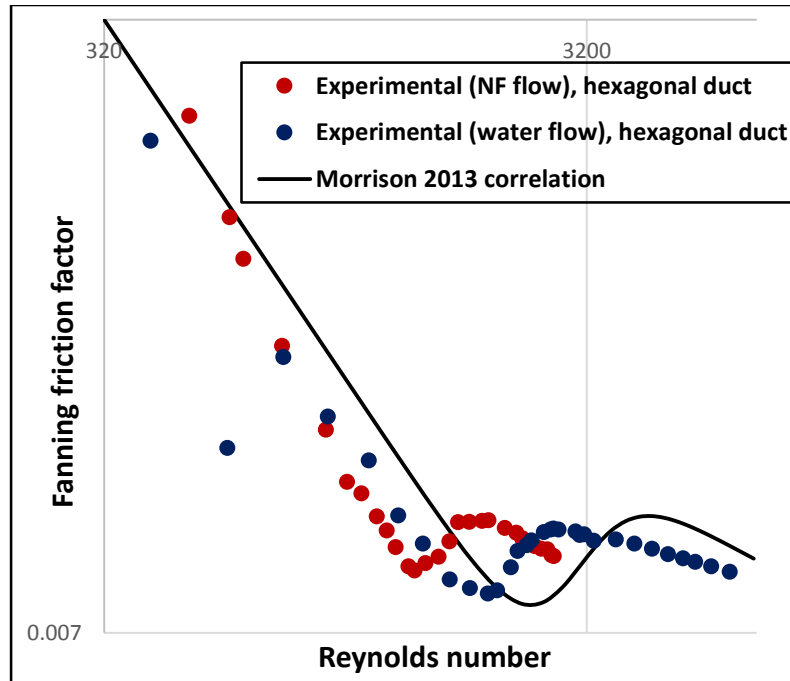
Figure 4.15 Comparison of the experimental friction factor with theoretical friction factor correlation vs. Reynolds number for water and NF flowing through the hexagonal duct.
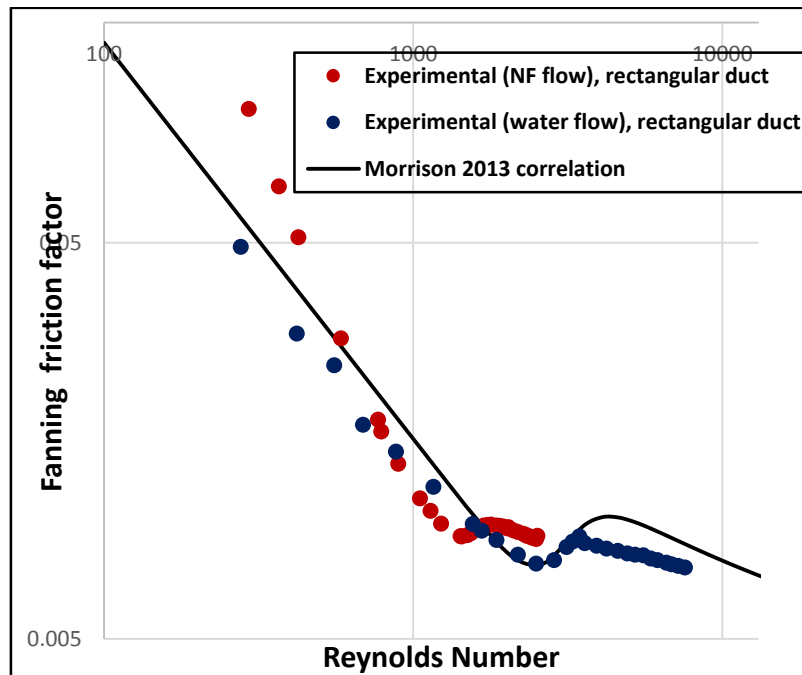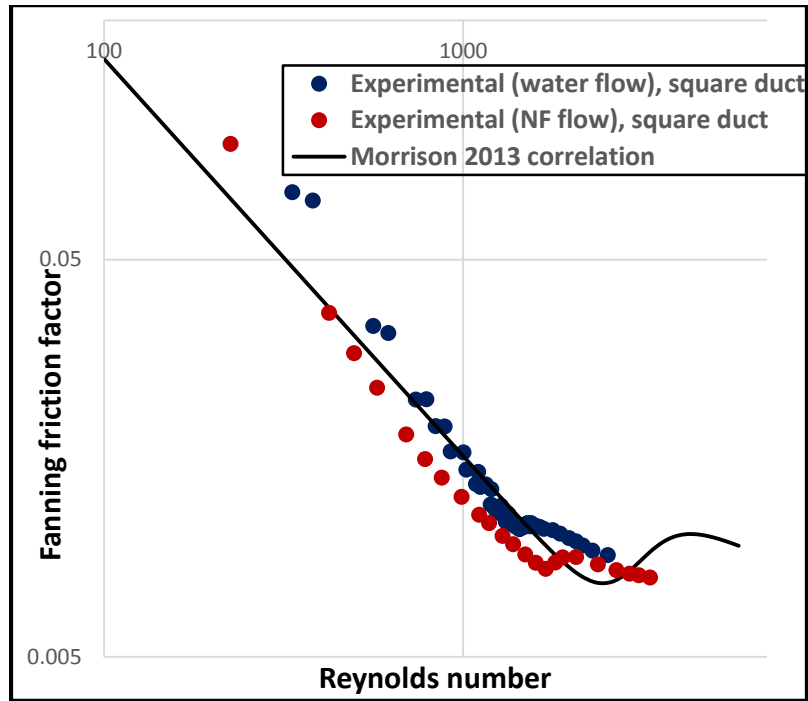

Figure 4.16 Comparison of the experimental friction factor with theoretical friction factor correlation vs. Reynolds number for water and NF flowing through the rectangular duct.

78

Figure 4.17 Comparison of the experimental friction factor with theoretical friction factor correlation vs. Reynolds number for water and NF flowing through the square duct.
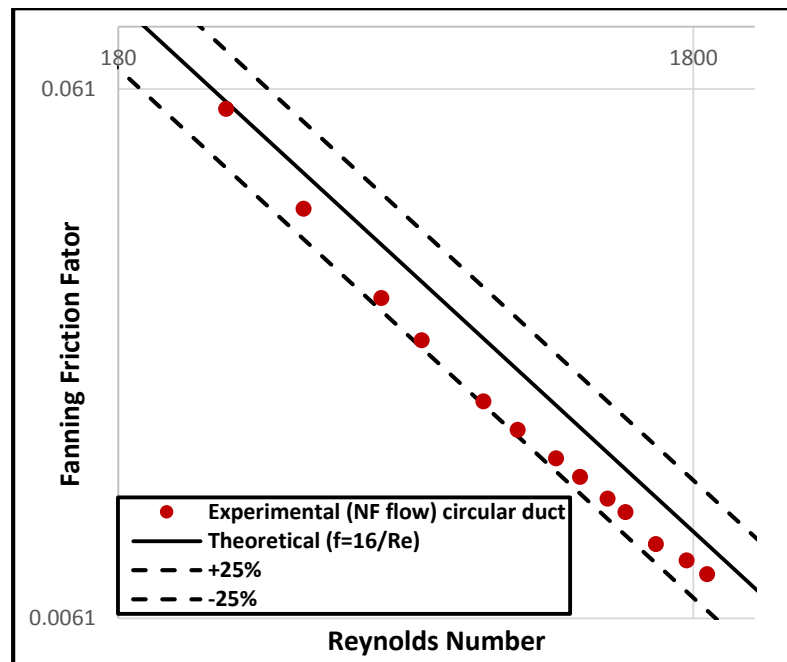

Figure 4.18 Comparison of the experimental friction factor and theoretical friction factor vs. Reynolds number for 9.58% by vol. silica/water nanofluid in circular duct.
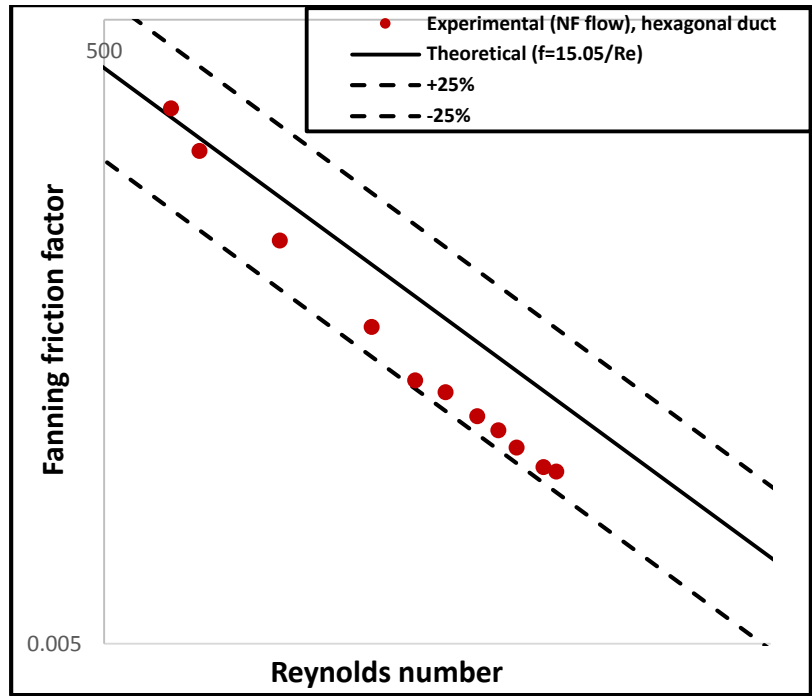
79

Figure 4.19 Comparison of the experimental friction factor and theoretical friction factor vs. Reynolds number for 9.58% by vol. silica/water nanofluid in hexagonal duct.
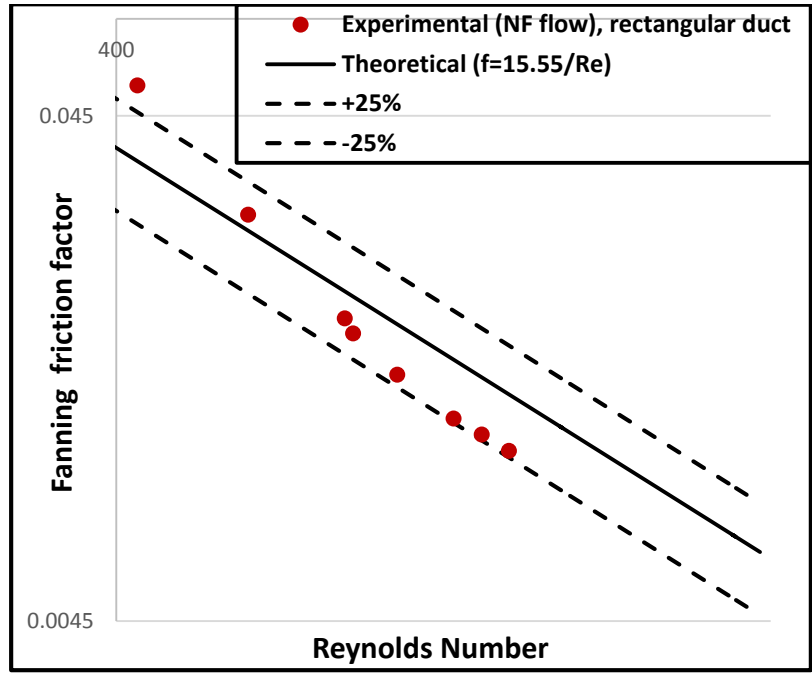

Figure 4.20 Comparison of the experimental friction factor and theoretical friction factor vs. Reynolds number for 9.58% by vol. silica/water nanofluid in rectangular duct.
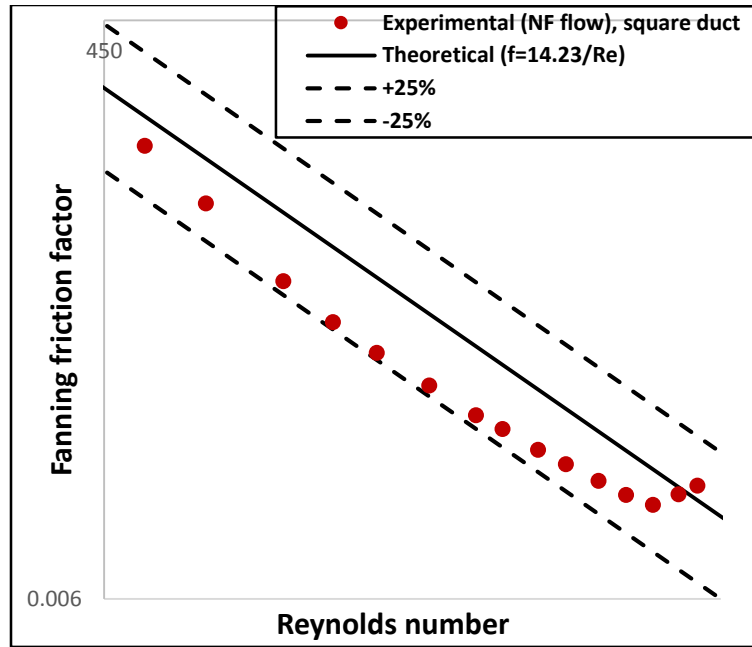
80

Figure 4.21 Comparison of the experimental friction factor and theoretical friction factor vs. Reynolds number for 9.58% by vol. silica/water nanofluid in square duct.
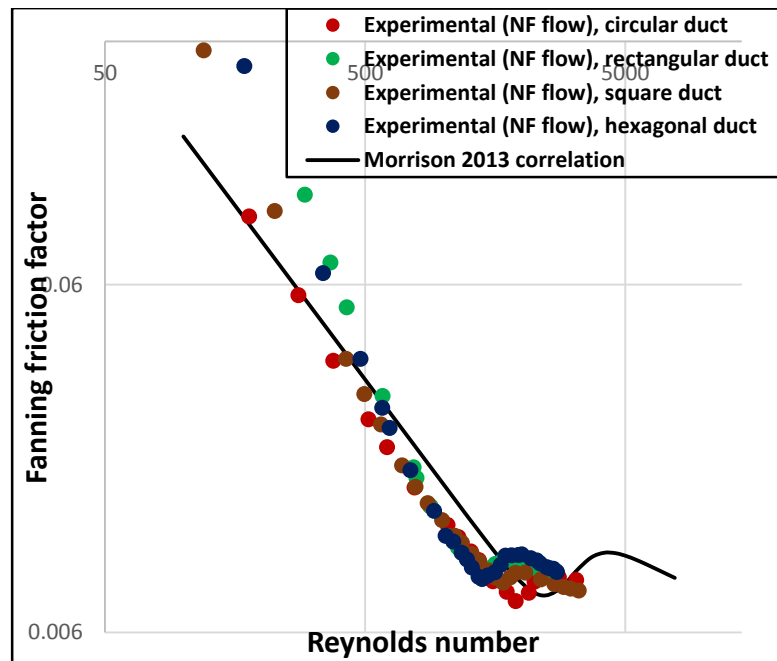

Figure 4.22 Comparison of the experimental friction factor and theoretical friction factor vs. Reynolds number for 9.58% by vol. silica/water nanofluid for all geometries.
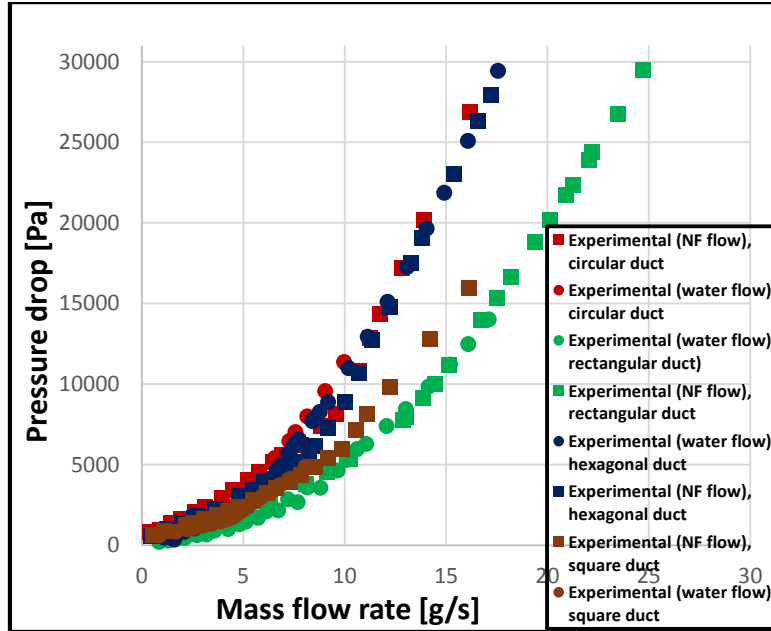
81

Figure 4.23 Plot comparing the experimental pressure drops for all duct geometries, NF flow.

4.5 Heat Transfer Results for the Nanofluid

The analysis of the heat transfer in a forced convection flow requires an understanding of the developing thermal entry length. For this analysis, the thermal entry given by (Lienhard & Lienhard, 2015) is employed, which is expressed mathematically as:

$$x_e \cong 0.034 Re_D Pr D_h \tag{4.19}$$

In Equation (4.19), x_e [m] is the entry length.

The heat transfer results of the nanofluid mostly lie in the laminar regime (although some ducts extended to the turbulent regime) and since this experiment is a constant heat flux condition such that the wall of the test sections is constantly heated and cooled so the heat flux from the wall to the fluid via convection remains constant and the bulk mean temperature of the nanofluid increases steadily at a fixed rate along the flow direction, a thermally fully developed flow was investigated. It has been established that the Nusselt number in a circular tube should be Nu = 4.36

82

for fully developed laminar flow under constant heat flux conditions. However, for this experiment the thermal profile did not reach fully developed condition since the total length of each duct was smaller than the thermal entry length. Therefore, the duct was too short to achieve thermally fully developed flow.

Figure 4.24 below compares the average Nusselt number vs. the Reynolds number for all the ducts with the intention of investigating which of the ducts give the best convective heat transfer behavior. The rectangular was observed to display the highest Nusselt number as the flow develops with increasing Reynolds number. This shows that the rectangular duct is a better convective heat transfer flow channel compared to the other channels.
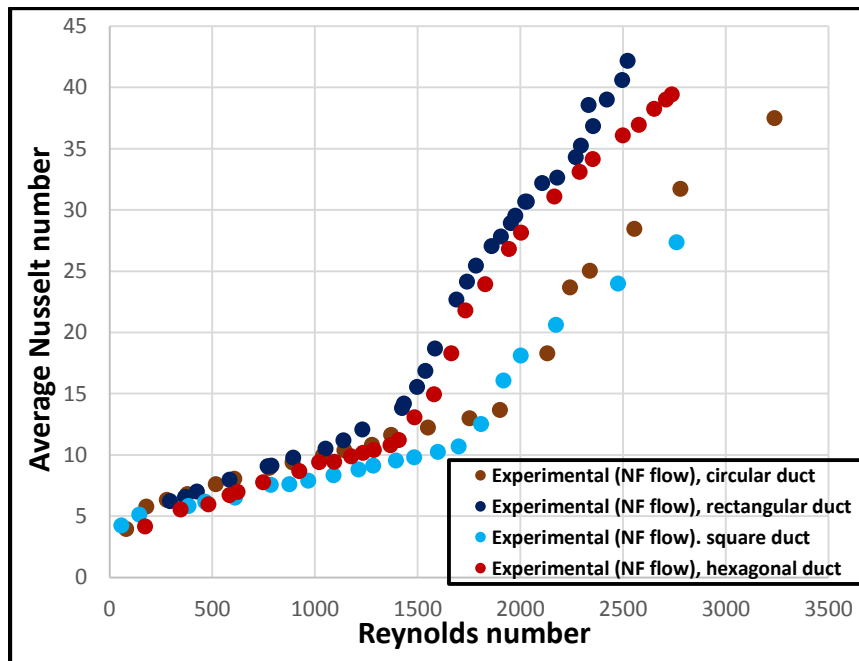

Figure 4.24 Plot comparing the average Nusselt number vs. Reynolds number for all ducts, NF flow.

In addition, the thermal performance of each fluid was investigated by plotting the average Nusselt number vs. the Reynolds separately for each duct geometry with the intention of comparing the convective heat transfer behavior of each fluid. These plots are shown in Figures

83

4.25 to 4.28 below. In all these figures, it was evident that the NF showed a higher Nusselt number compared to the water at all points in the flow. This confirms the claim from literature that NF is a better heat transfer medium compared to water.
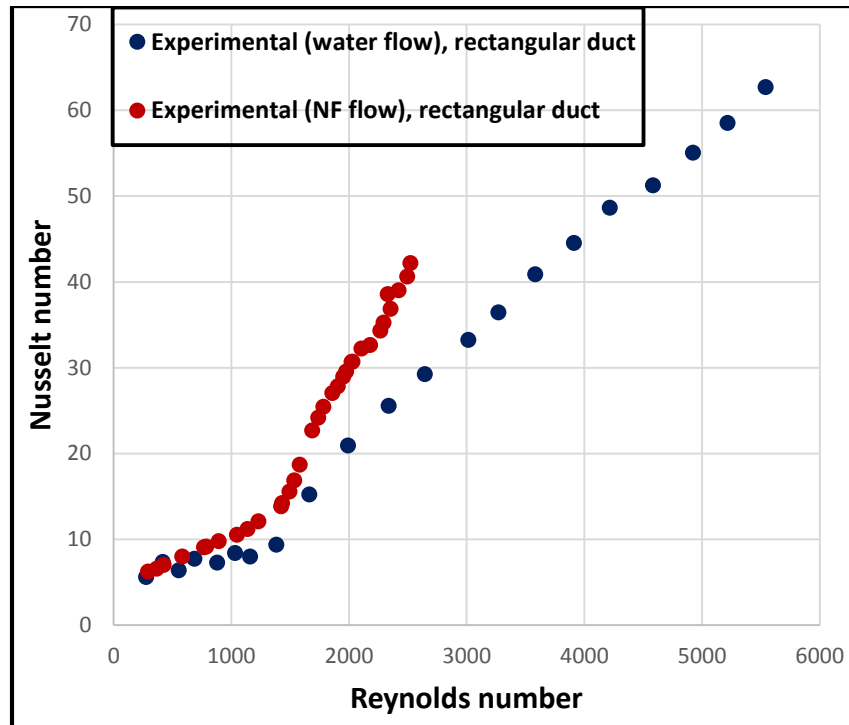

Figure 4.25 Plot comparing the experimental Nusselt number for water and NF in the rectangular duct.
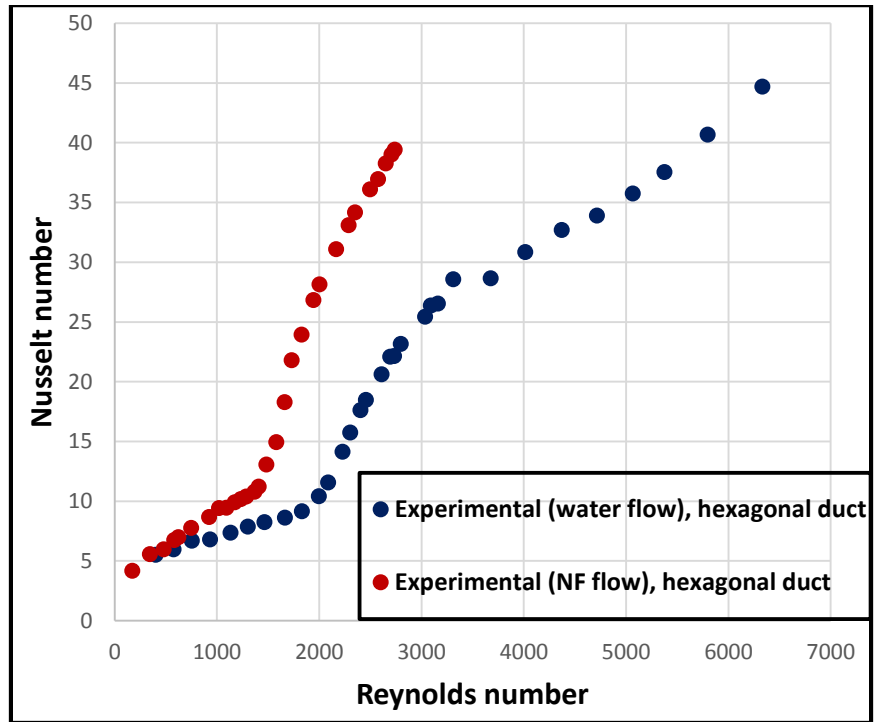
Figure 4.26 Plot comparing the experimental Nusselt number for water and NF in the hexagonal duct.
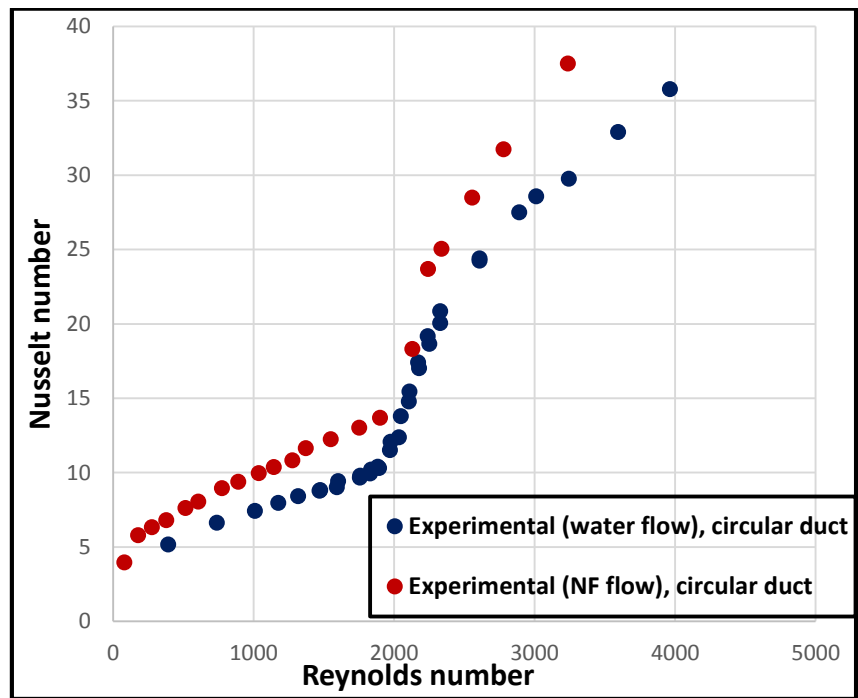

Figure 4.27 Plot comparing the experimental Nusselt number for water and NF flow through the circular duct.

85
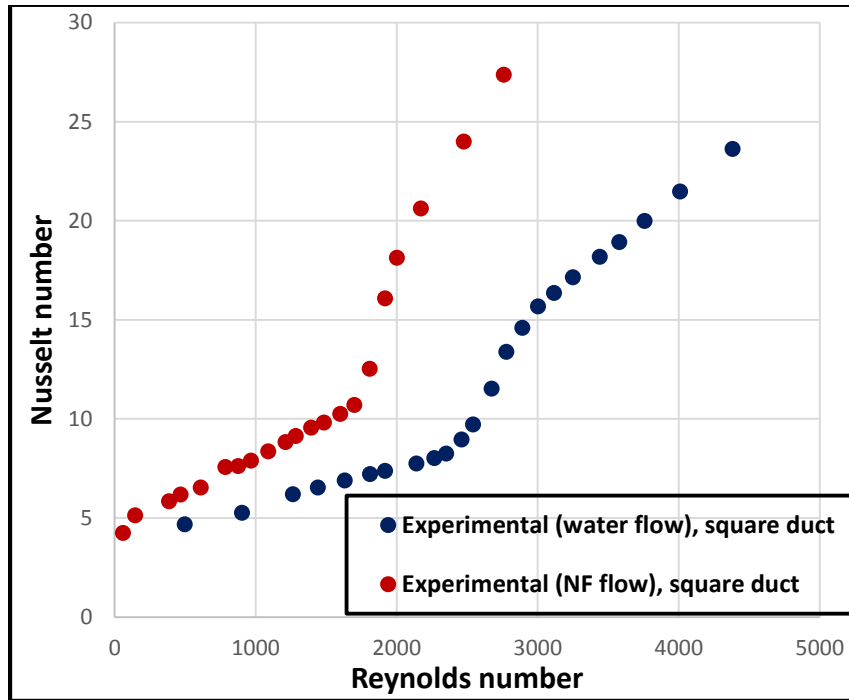
Figure 4.28 Plot comparing the experimental Nusselt number of water and NF in the square duct.

The Lienhard & Lienhard (2012) correlation given by Equation (4.15) was also used to predict the experimental Nusselt number for the thermally developing flow in the laminar regime for the NF. Figures 4.29 to 4.32 show the plots of the experimental Nusselt number vs. the dimensionless distance (x^+) from which it was observed that all the experimental values lie within $\pm 20\%$ of the values predicted by the Lienhard & Lienhard (2012) correlation. This show that the conventional correlation for single phase Newtonian fluids can satisfactorily predict the heat transfer behavior of non-Newtonian colloidal suspensions.

Figure 4.29 Nusselt number vs. dimensionless distance for 9.58% vol. silica/water NF flowing through a heated hexagonal duct.

Figure 4.30 Nusselt number vs. dimensionless distance for 9.58% vol. silica/water NF flowing through a heated rectangular test section.
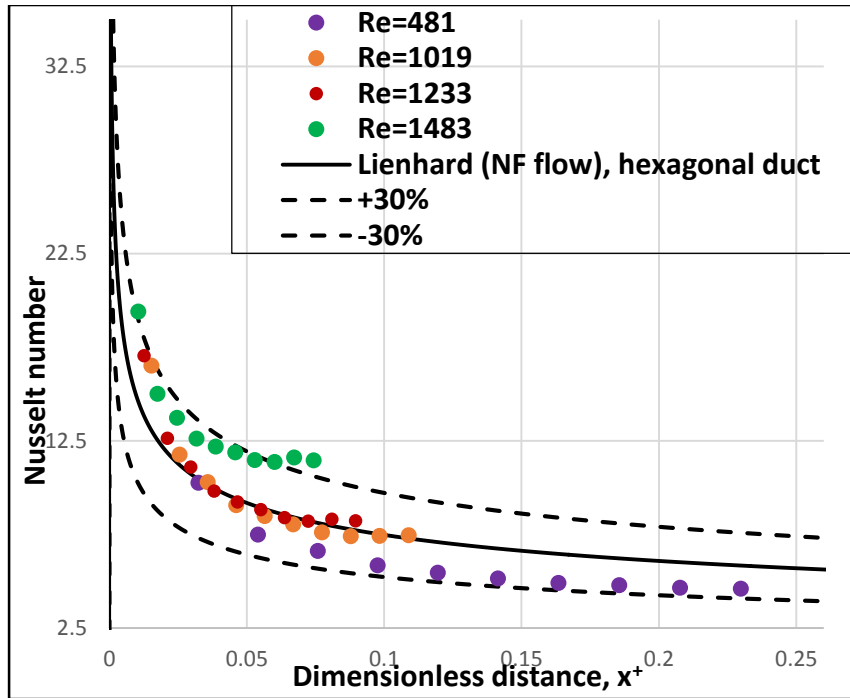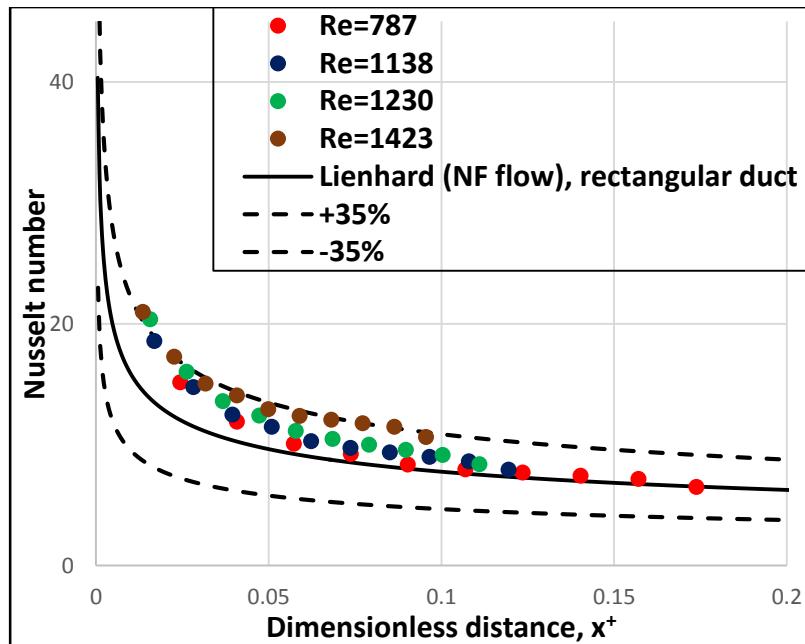
87
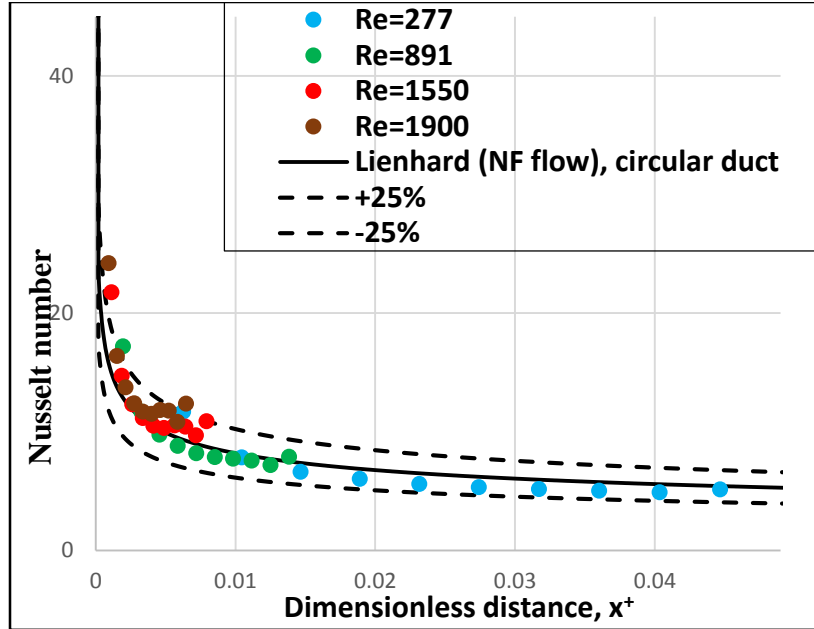
Figure 4.31 Nusselt number vs. dimensionless distance for 9.58% vol. silica/water NF flowing through a heated circular test section.
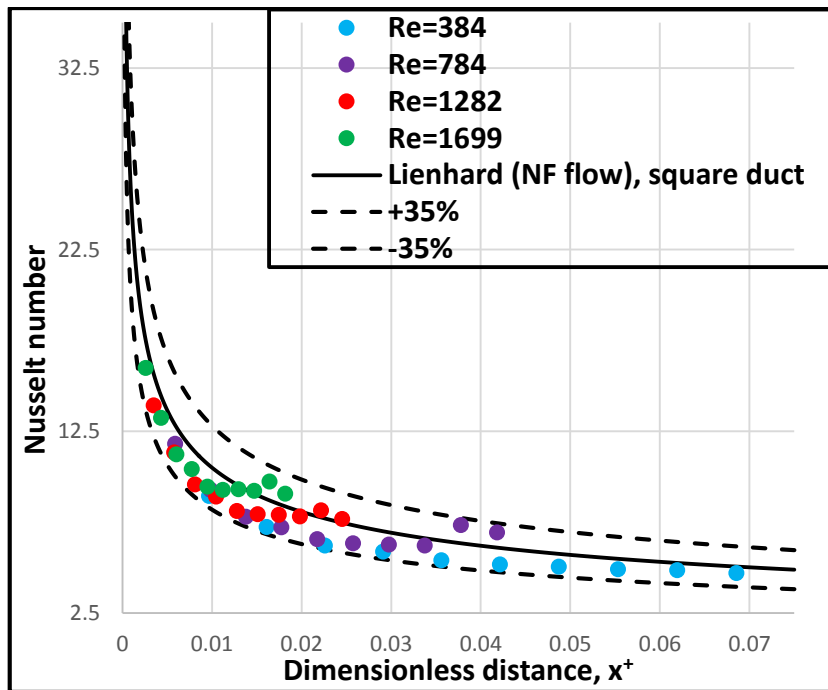
Figure 4.32 Nusselt number vs. dimensionless distance for 9.58% vol. silica/water NF flowing through a heated square test section.

88

Also, the heat transfer performance of each duct geometry was investigated for the NF and water at same Reynolds number and axial distance of 4.5 inch along the length of the tube. The Figure 4.33 below compares the local Nusselt number vs the Reynolds number at a local axial distance of 4.5 in. At equal Reynolds number of approximately 2000, it can be observed that the rectangular cross-section have highest value of Nusselt numbers compared to the other geometries while the square duct was observed to have the lowest value of Nusselt number at the same Reynolds number. This observation shows that the rectangular duct gives a better thermal performance compared to the other ducts.
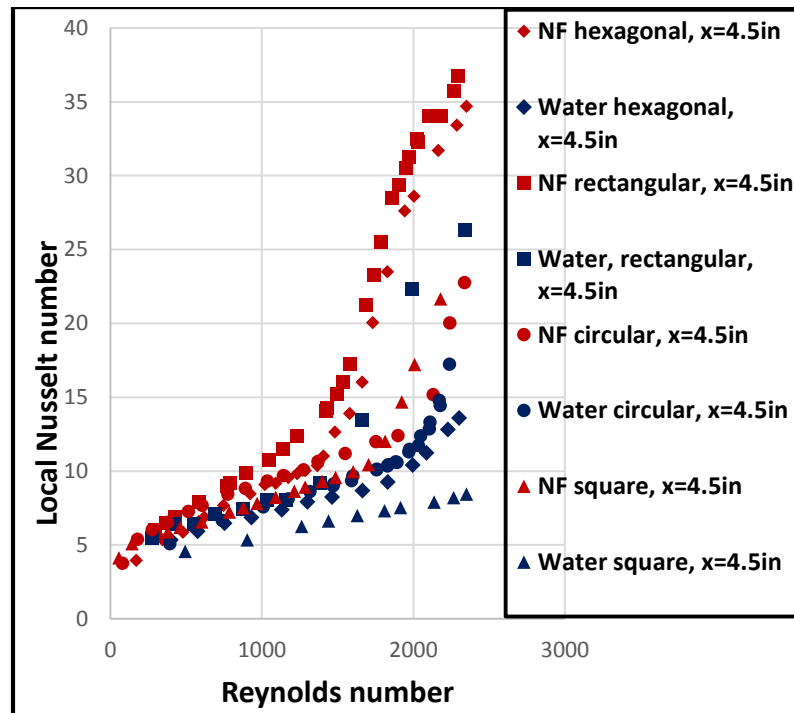
Figure 4.33 Comparison of the Nusselt number vs. Reynolds numbers for water and NF at a local axial distance of x=4.5in for all duct geometries.

4.5.1 Convective Heat Transfer Coefficient

The addition of nanoparticles to base fluid was proven to increase the heat transfer potential of nanofluids and this was also checked for all the four test sections. With the assumption that the losses are negligible, the heat transfer coefficient is calculated from the electrical energy supplied using the following relations:

$$Q = V * I \tag{4.20}$$

$$h = \frac{Q}{A\,(T_s - T_b)} \tag{4.21}$$

In Equation (4.21), $\;T_b = (T_i + T_o)/2$ (4.22)

The plot of the average heat transfer coefficient vs Reynolds number for the different duct geometries is shown in Figure 4.34. Interestingly, the heat transfer coefficient of the NF was higher than that of water for all the duct geometries at values of Reynolds number and this observation is consistent with literature which further confirms that the presence of nanoparticles caused an enhancement in heat transfer coefficients in the nanofluid. However, the rectangular and hexagonal ducts showed the highest overall heat transfer coefficient. The same observation was seen when all the ducts geometries are compared for NF flow only as shown in Figure 4.35 below.

Figure 4.34 Comparison of the overall heat transfer coefficient vs. Reynolds numbers for water and NF flowing through all duct geometries.

Figure 4.35 Comparison of the overall heat transfer coefficient vs. Reynolds numbers for the NF flowing through all duct geometries.

91

In addition, the heat transfer coefficient of the NF and water was investigated at a local axial distance of 5.5 in as shown in Figure 4.36 for all the duct geometries. It was also obvious that the NF showed a higher heat transfer coefficient compared to water and the rectangular showed the highest value of heat transfer coefficient.
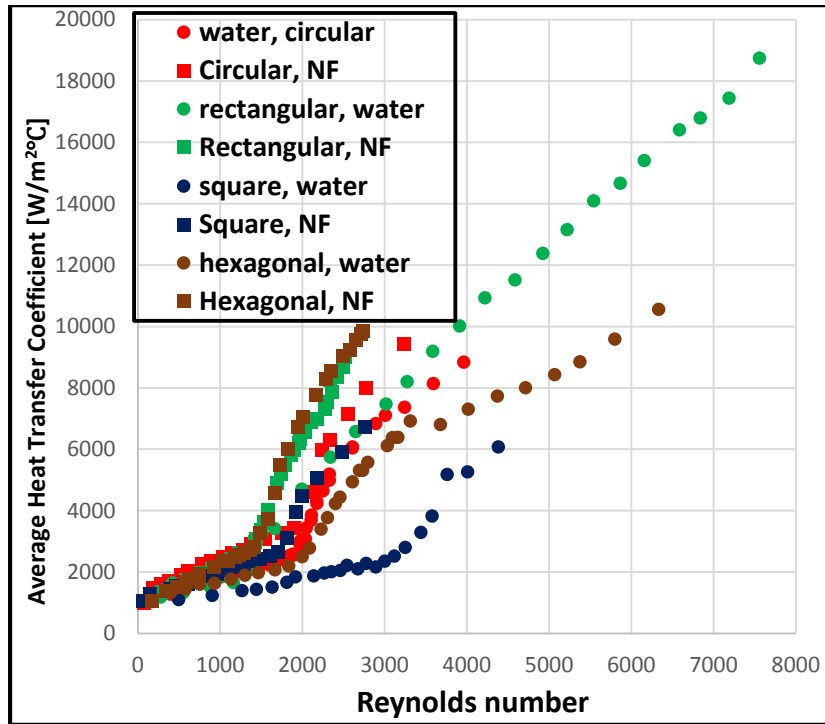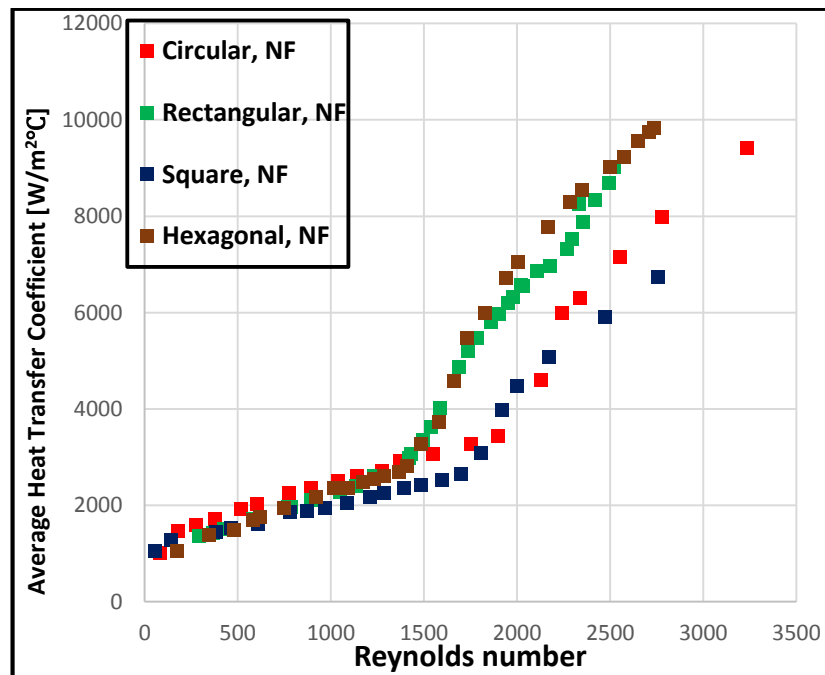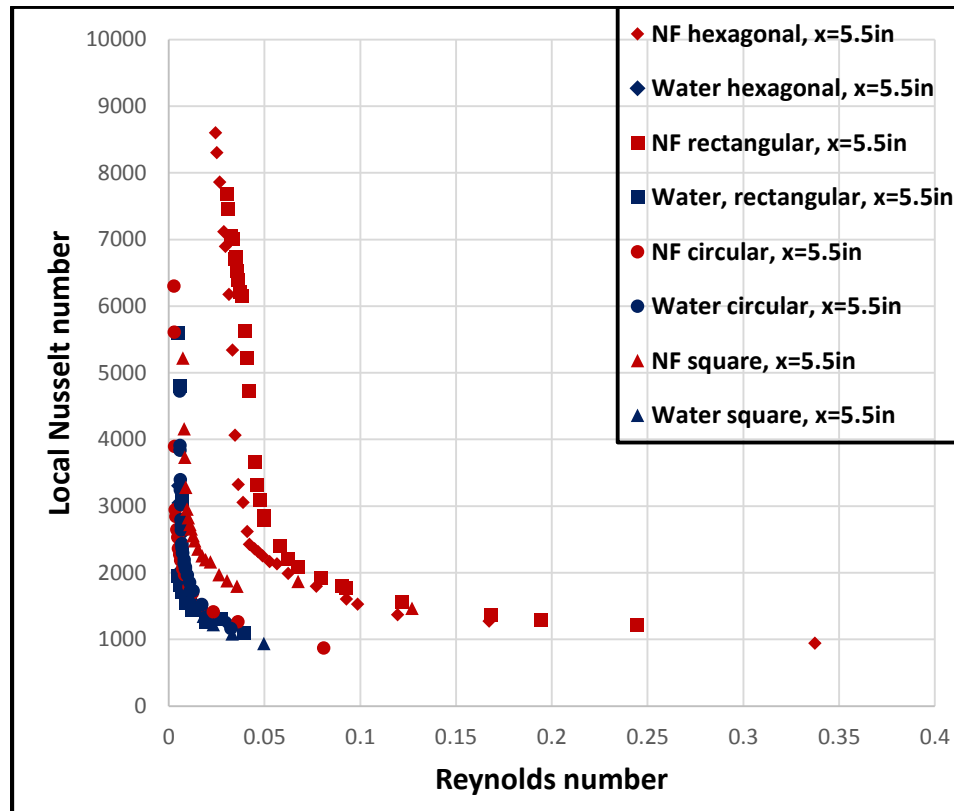

Figure 4.36 Comparison of the overall heat transfer coefficient vs. Reynolds numbers for the NF flowing through all duct geometries.

CHAPTER V

CONCLUSIONS AND RECOMMENDATIONS

In this chapter, some of the observations from the result of this research in comparison with other available results from literature will be discussed. Ultimately, some final conclusions and recommendations for future research efforts in this line will be made.

5.1 Conclusions

The results of the convective heat transfer properties and pressure drop characteristics of silica/water nanofluids of 9.58% by volume concentration was experimentally investigated and the result was compared for rectangular, hexagonal, square and circular test sections. The following are some of the conclusions reached:

The measured data for the thermal conductivity of the nanofluid and water was analyzed and compared with existing standard values from the literature. As expected, and it was observed that there is an obvious increase in thermal conductivity of the NF based on the addition of silica nanoparticles to water, i.e. nanofluid exhibited a slightly higher better thermal conductivity of 1.5% to 4.25% compared to water. The experimental values for the viscosity of the NF were compared with that of water. It was observed that the viscosity of NF was higher than that of water which is the base fluid. Based on the available data, it was observed that the NF is shear thickening non-Newtonian fluid at 9.58% by volume concentration and the viscosity of the NF was estimated based on the power law for non-Newtonian fluids.

93

In addition, the friction factor of the NF in the laminar region can be well approximated by the Darcy-Weisbach equation developed for single phase fluids. Although the addition of nanoparticles slightly improves the convective heat transfer behavior of the base fluid but no significant change in the friction factor of both fluids was observed. Therefore, it can be concluded that the NF behaves as a conventional single phase base fluid in the laminar regime. The NF was observed to reach transition earlier which could be traced to the presence of nanoparticles causing the particle migration to the boundary layer thereby generating eddies in the boundary layer. Friction factor decreases with increasing Reynolds number for both fluids because increasing the Reynolds number reduces the pipe wall viscous drag force and the pressure drop.

For the NF, improvement in heat transfer is higher at the thermal entrance region which is consistent with literature. Also, conventional correlations for single phase fluid can also be used for the NF to predict heat transfer performance. For instance, the correlation given by Lienhard & Lienhard (2015) was in good agreement with the measured values of Nusselt number for a thermally developing flow. Hence, the heat transfer of nanofluids can be accurately predicted by the correlation given for a single phase fluids in the laminar regime.

The heat transfer coefficient of the NF was better than that of water when compared at same dimensionless distance and Reynolds number. This is also true for the Nusselt number comparison of the NF and water. Also, the decay of Nusselt number is more rapid for the nanofluid which shows that that the dispersion of nanoparticle affects the development of the thermal boundary layer.

5.2 Recommendations

Due to the sensitivity of thermophysical properties, some errors might have affected the recorded data owing to disturbances produced by vibration and sound from the surrounding. If these disturbances can be eliminated or at least minimized, a better result should be achieved.

Due to the limitation of the small rating of the pump used to supply pressure, a fully turbulent flow could not be achieved for most of the ducts when the NF was passed through the ducts. As a result, the friction factor and heat transfer results for the nanofluid was measured mostly in the laminar region. Hence, it is necessary to secure a pump of higher ratings which is capable of generating turbulent flow in the test sections for the nanofluid in order to adequately study the friction factor and heat transfer behavior in the turbulent region.

The effect of increasing nanoparticle concentration should be investigated for each duct geometry. This is necessary in order to determine the optimal concentration at which heat transfer is stilled enhanced through the use of the nanofluid and also to determine the concentration at which the NF seizes to behave as a Newtonian fluid. Different nanofluids made from varying materials, particle shapes, particles sizes and concentrations should be investigated.

Nanofluids made from liquid base fluids have been extensively studied for their capacities to increase the heat transfer rate compared with conventional fluids. In similar vein, the base fluid can be changed to gases that would dissolve in the nanofluid and following similar procedure, the heat transfer enhancement capability of the nanofluid-gas mixture may be investigated. An example of a gas to consider is air. A test section of better length should be utilized because the length of the test section for this experiment was 12 inches which is too short to investigate

95

thermally fully developed flow in the laminar region. However, increase in length requires significant pumping power.

REFERENCES

Abreu, B. et al., 2014. Experimental characterization of convective heat transfer with MWCNT based nanofluids under laminar flow conditions. *Heat and Mass Transfer,* Volume 50, pp. 65-74.

Alvarado, J. L. et al., 2007. Thermal Performance of Microencapsulated Phase Change Material Slurry in Turbulent Flow under Constant Heat Flux. *International Journal of Heat and Mass Transfer,* p. 1938–1952.

Anoop, K. B., Sundararajan, T. & Das, S. K., 2009. Effect of particle size on the convective heat transfer in nanofluid in the developing region. *International Journal of Heat and Mass Transfer,* Volume 52, p. 2189–2195.

Asirvatham, L. G., Vishal, N., Gangatharan, S. K. & Lal, D. M., 2009. Experimental study on forced convective heat transfer with low volume fraction of CuO/water nanofluid. *Energies,* 2(1), pp. 97-119.

Cengel, Y. A., 2007, Heat and Mass Transfer: A Practical Approach. 3rd edition New York: McGraw Hill.

Chein, R. & Chuang, J., 2007. Experimental Microchannel Heat Sink Performance Studies using Nanofluids. *International Journal of Thermal Sciences,* 46(1), pp. 57-66.

Choi, S. S. et al., 2001. Anomalous Thermal Conductivity Enhancement in Nanotube Suspensions. *Applied Physics Letters,* 79(14), pp. 2252-2254.

Choi, S. U. S. & Eastman, J. A., 1995. *Enhancing Thermal Conductivity of Fluids with Nanoparticles.* San Francisco, CA., s.n.

Cristina, B., Ivan, I. P. & Kevin, R., 2007. *Nanomaterials and nanoparticles: Sources and toxicity,* Ontario: Department of Physics, Queen's University.

Das, S. K., Choi, S. S., Yu, W. & Pradeep, T., 2007. *Nanofluids: Science & Technology.* 1st ed. s.l.:Wiley-Interscience.

Das, S. K., Putra, N. & Thiesen, P., 2003. Temperature Dependence of Thermal Conductivity Enhancement for Nanofluids. *Journal of Heat Transfer ASME,* Volume 125, pp. 567-574.

Ding, Y., Alias, H., Wen, D. & Williams, R. A., 2006. Heat transfer of aqueous suspensions of carbon nanotubes (CNT nanofluids). *International Journal of Heat and Mass Transfer,* Volume 49, pp. 240-250.

Eastman, J. A., Choi, S.U.S., Li, S., Thompson, L. J., and Lee, S., (1996). Enhanced Thermal Conductivity through the Development of Nanofluids. MRS Proceedings, 457, 3 doi:10.1557/PROC-457-3.

Eastman, J. A. et al., 2001. Anomalously Increased Effective Thermal Conductivities of Ethylene Glycol-Based Nanofluids Containing Copper Nanoparticles. *Applied Physics Letter,* 78(6), pp. 718-720.

Ebrahimi, M., Farhadi, M., Sedighi, K. & Akbarzade, S., 2014. Experimental investigation of force convection heat transfer in a car radiator filled with SiO2–water nanofluid. *International Journal of Engineering,* Volume 27, pp. 333-340.

Fotukian, S. M. & Esfahany, M. N., 2010. Experimental study of turbulent convective heat transfer and pressure drop of dilute CuO/water nanofluid inside a circular tube. *International Communications in Heat and Mass Transfer,* 37(2), pp. 214-219.

Gireesha, B. J. & Rudraswamy , N. G., 2014. Chemical reaction on MHD flow and heat transfer of a nanofluid near the stagnation point over a permeable stretching surface with non-uniform heat source/sink. *International Journal of Engineering, Science and Technology,* Volume 6, pp. 13-25.

Guo, S. Z., Li, Y., Jiang, J. S. & Xie, H. Q., 2010. Nanofluids Containing gamma-Fe2O3 Nanoparticles and Their Heat Transfer Enhancements. *Nanoscales Research Letters,* 5(7), pp. 1222-1227.

Haghighi, E. B. et al., 2014. Experimental study on convective heat transfer of nanofluids in turbulent flow: Methods of comparison of their performance. *Experimental Thermal and Fluid Science ,* Volume 57, p. 378–387.

Hamilton, R. L. & Crosser, O. K., 1962. Thermal conductivity of heterogeneous two- component systems. *Industrial and Engineering Chemistry Fundamentals,* 1(3), pp. 187-191.

He., Y. et al., 2007. Heat transfer and flow behavior of aqueous suspensions of TiO2 nanoparticles (nanofluids) flowing upward through a vertical pipe. *International Journal of Heat and Mass Transfer,* Volume 50, p. 2272–2281.

Heris, S. Z., Esfahany, M. N. & Etemad, S., 2007. Experimental Investigation of Convective Heat Transfer of Al Nanofluids in Fully Developed Laminar Flow Regime. *International Journal of Heat and Mass Transfer,* Volume 52, pp. 193-199.

Heris, S. Z., Etemad, S. & Esfahany, M. N., 2006. Experimental Investigation of Oxide Nanofluids Laminar Flow Convective Heat Transfer. *International Communications in Heat and Mass Transfer ,* Volume 33, p. 529–535.

Heyhat, M. M., Rashidi, A. M., Momenpour, M. H. & Amrollahi, A., 2013. Experimental investigation of laminar convective heat transfer and pressure drop of water-based Al2O3 nanofluids in fully developed flow regime. *Experimental Thermal and Fluid Science,* Volume 44, p. 483–489.

Huaqing, X., Wei, Y., Yang, L. & Lifei, C., 2011. Discussion on the thermal conductivity enhancement of nanofluids. *Nanoscale Research Letters,* 6(1), p. 124.

Hwang, K. S., Jang, S. P. & Choi, S. S., 2009. Flow and convective heat transfer characteristics of water-based Al2O3 nanofluids in fully developed laminar flow regime. *International Journal of Heat and Mass Transfer ,* Volume 52, pp. 193-199.

Jahanshahi, M. et al., 2010. Numerical simulation of free convection based on experimental measured conductivity in a square cavity using Water/SiO2 nanofluid. *International Communications in Heat and Mass Transfer,* 37(6), p. 687–694.

Jeong, J. et al., 2013. Particle shape effect on the viscosity and thermal conductivity of ZnO nanofluids. *International Journal of Refrigeration,* Volume 36, pp. 2233-2241.

Kakac, S., Bergles, A. E. & Mayinger, F., 1981. *Heat Exchangers, Thermal-Hydraulic Fundamentals and Design.* New York: McGraw Hill.

Kaufui, V. W. & Omar, D. L., 2010. Applications of Nanofluids: Current and Future.. *Advances in Mechanical Engineering,* Volume 2010, pp. 1-11.

Kayhani, M. H. et al., 2012. Experimental study of convective heat transfer and pressure drop of TiO2/water nanofluid. *International Communications in Heat and Mass Transfer,* Volume 39, p. 456–462.

Keblinski, P., Phillpot, S. R., Choi, S. S. & Eastman, J. A., 2002. Mechanisms of Heat Flow in Suspensions of Nano-Sized Particles (Nanofluids). *Int. J. Heat Mass Tran,* 45(4), pp. 855-863.

Khodadadi, J. M. & Hosseinizadeh, S. F., 2007. Nanoparticle-enhanced phase change materials (NEPCM) with great potential for improved thermal energy storage. *International Communications in Heat and Mass Transfer,* 34(5), p. 534–543.

Kole, M. & Dey, T. K., 2012. Thermophysical and pool boiling characteristics of ZnO-ethylene glycol nanofluids. *International Journal of Thermal Sciences,* Volume 62, pp. 61-70.

Kulkarni, D. P., Vajjha, R. S., Das, D. K. & Oliva, D., 2008. Application of aluminum oxide nanofluids in diesel electric generator as jacket water coolant. *Applied Thermal Engineering,* Volume 28, pp. 1774-1781.

Kwak, K. & Kim, C., 2005. Viscosity and thermal conductivity of copper oxide nanofluid dispersed in ethylene glycol. *Korea-Australia Rheology Journal,* Volume 17, pp. 35-40.

Lazarus, G., Raja, B., Mohan, D. L. & Wongwises, S., 2010. Enhancement of heat transfer using nanofluids-An overview.. *Renewable and Sustainable Energy Reviews,* 14(2), pp. 629-641.

Lee, J. & Mudawar, I., 2007. Assessment of the Effectiveness of Nanofluids for Single-Phase and Two-Phase Heat Transfer in Micro-Channels. *Int. J. Heat Mass Tran.,* 50(3-4), pp. 452-463.

Lee, S., Choi, S. S., Li, S. & Eastman, J. A., 1999. Measuring thermal conductivity of fluids containing oxide nanoparticles. *Journal of Heat Transfer,* Volume 121, pp. 280-288.

Lelea, D., 2010. Effects of temperature dependent thermal conductivity on Nu number behavior in micro-tubes. *International Communication in Heat and Mass Transfer,* Volume 37, p. 245–249.

Lienhard, J. H. I. & Lienhard, J. H. V., 2012. *A Heat Transfer Textbook.* 4 ed. Cambridge, MA: Phlogiston Press.

Li, Q. & Xuan, Y., 2002. Convective Heat Transfer and Flow Characteristics of Cu-Water Nanofluid. *Science China Series E,* 45(4), pp. 408-416.

Liu, M. S., Lin, M. C., Huang, I. T. & Wang, C. C., 2006. Enhancement of thermal conductivity with CuO for Nanofluids. *Chemical Engineering and Technology,* Volume 29, pp. 72-77.

Liu, Z. G., Liang, S. Q. & Takei, M., 2007. Experimental study on forced convective heat transfer characteristics in quartz microtube. *International Journal of Thermal Science,* Volume 46, p. 139–148.

Lotfi, R., Saboohi, Y. & Rashidi, A. M., 2010. Numerical study of forced convective heat transfer of nanofluids: comparison of different approaches. *International Communications in Heat and Mass Transfer,* 37(1), pp. 74-78.

Maiga, S. B., Nguyen, C. T., Galanis, N. & Roy, G., 2004. Heat transfer behaviors of nanofluids in a uniformly heated tube. *Superlattices and Microstructures,* Volume 35, p. 543–557.

Metzner, A. B. & Reed, J. C., 1955. Flow of Non-Newtonian Fluids-Correlation of the Laminar, Transition, and Turbulent-flow Regions. *American Insitute of Chemical Engineers,* pp. 434-440.

Meyer, J. P., Mehrabi, M. & Sharifpur, M., 2013. Modelling and multi-objective optimisation of the convective heat transfer characteristics and pressure drop of low concentration TiO2–water nanofluids in the turbulent flow regime.. *International Journal of Heat and Mass Transfer,* Volume 67, pp. 646-653.

Minea, A. A., 2013. Effect of microtube length on heat transfer enhancement of a water/Al2O3 nanofluid at high Reynolds numbers. *Heat and Mass Transfer,* Volume 62, p. 22–30.

Morrison, F. A., 2013. "Data Correlation for Friction Factor in Smooth Pipes," Department of Chemical Engineering, Michigan Technological University, Houghton, MI; http://www.chem.mtu.edu/~fmorriso/DataCorrelationForSmoothPipes2013.pdf

Mojarrad, M. S., Keshavarz, A., Ziabasharhagh, M. & Raznahan, M. M., 2014. Experimental investigation on heat transfer enhancement of alumina/water and alumina/water–ethylene glycol nanofluids in thermally developing laminar flow. *Experimental Thermal and Fluid Science ,* Volume 53, p. 111–118.

Murshed, S. S., Leong, K. C. & Yang, C., 2005. Enhanced thermal conductivity of TiO2/water based nanofluids. *International Journal of Thermal Science ,* Volume 44, pp. 367-373.

Namburu, P. K., Das, D. K., Tanguturi, K. M. & Vajjha, R. S., 2009. Numerical study of turbulent flow and heat transfer characteristics of nanofluids considering variable properties. *International Journal of Thermal Sciences,* 48(2), p. 290–302.

Nguyen, C. T., Roy, G., Gauthier, C. & Galanis, N., 2007. Heat transfer enhancement using Al2O3/water nanofluid for electronic liquid cooling system. *Applied Thermal Engineering,* Volume 28, p. 1501–1506.

Pak, B. & Cho, Y., 1998. Hydrodynamic and heat transfer study of dispersed fluids with submicron metallic oxide particles. *Experimental Heat Transfer,* Volume 11, pp. 151-162.

Pawel, K., Jeffrey, A. & David, G. C., 2005. Nanofluids for thermal transport. *Materials today,* Volume 8, pp. 36-44.

Ramires, M. V. et al., 1994. *Standard Reference Data for the Thermal Conductivity of Water,* s.l.: International Union of Pure & Applied Chemistry.

Romano, J. M., Parker, J. C. & Ford, Q. B., 1997. Application Opportunities for Nanoparticles Made from the Condensation of Physical Vapors. *Adv. Pm. Part.,* Volume 130, pp. 12-13.

Rostamani, M., Hosseinizadeh, S. F., Gorji, M. & Khodadadi, J. M., 2010. Numerical study of turbulent forced convection flow of nanofluids in a long horizontal duct considering variable properties. *International Communications in Heat and Mass Transfer ,* Volume 37, p. 1426–1431.

Sahin, A. Z., 1998. Irreversibilities in various duct geometries with constant wall heat flux and laminar flow. *Energy,* 23(6), p. 465–473.

Salman, B. H., Mohammed, H. A. & Kherbeet, A. S., 2014. Numerical and experimental investigation of heat transfer enhancement in a microtube using nanofluids. *International Communications in Heat and Mass Transfer,* Volume 59, p. 88–100.

Shah, R. K. & London, A. L., 1978. *Laminar Flow Forced Convection in Ducts.* New York: Academic Press.

Sharif, Md. T., 2015. Experimental Investigation of Thermophysical Properties, Pressure Drop and Heat Transfer of Non-Newtonian Silica Colloid Flow in Tubes, M.S Thesis, University of North Dakota, Grand forks, North Dakota, USA.

Sommers, A., 2012. *Sommers Research Group.* [Online]
Available at: http://www.users.miamioh.edu/sommerad/research.html
[Accessed 3 March 2015].

Sommers, A. D. & Yerkes, K. L., 2010. Experimental investigation into the convective heat transfer and system-level effects of Al2O3-propanol nanofluid. *Journal of Nanoparticle Research,* Volume 12, pp. 1003-1014.

Sundar, L. S., Singh, M. K., Bidkin, I. & Sousa, A. M., 2014. Experimental investigations in heat transfer and friction factor of magnetic Ni nanofluid flowing in a tube. *International Journal of Heat and Mass Transfer,* Volume 70, pp. 224-234.

Tiwari, S., 2012. *Evaluation of Thermophysical Properties, Friction Factor and Heat Transfer of Alumina Nanofluid Flow in Pipes, M.S Thesis, University of North Dakota, Grand forks, North Dakota, USA.*

Tsai, C. Y. et al., 2004. Effect of structural character of gold nanoparticles in nanofluid on heat pipe thermal performance. *Materials letters,* 58(9), p. 1461–1465.

Vajjha, R. S. & Das, D. K., 2009. Experimental Determination of Thermal Conductivity of Three Nanofluids and Development of New Correlations. *International Journal of Heat & Mass Transfer,* Volume 52, pp. 4675-4682.

Visinee, T. & Somchai, W., 2010. Critical review of heat transfer characteristics of Nanofluids. *Renewable and Sustainable Energy Reviews,* Volume 11, pp. 512-523.

Wang, B. X., Sheng, W. Y. & Peng, X. F., 2009. A novel statistical clustering model for predicting thermal conductivity of Nanofluids. *International Journal of Thermophysics, 30, pp.,* Volume 30, pp. 1992-1998.

Wang, B., Zhou, L. & Peng, X., 2003. A Fractal Model for Predicting the Effective Thermal Conductivity of Liquid with Suspension of Nanoparticles. *Int. J. Heat Mass Tran.,* 46(14), pp. 2665-2672.

Wang, X.-j., Li, X. & Yang, S., 2009. Influence of pH and SDBS on the Stability and Thermal Conductivity of Nanofluids. *Energy & Fuels ,* Volume 23, p. 2684–2689.

Wang, X. Q. & Mujumdar, A. S., 2007. Heat transfer characteristics of nanofluids: a review. *International Journal of Thermal Sciences,* Volume 46, pp. 1-19.

Webb, R. L. & Kim, N. H., 2005. *Principles of Enhanced Heat Transfer.* New York: Taylor and Francis.

Wei, Y. & Huaqing, X., 2012. A Review on Nanofluids: Preparation, Stability Mechanisms, and Applications. *Journal of Nanomaterials,* Volume 2012.

Wen, D. & Ding, Y., 2004. Experimental investigation into convective heat transfer of nanofluids at the entrance region under laminar flow conditions. *International Journal of Heat and Mass Transfer ,* Volume 47, p. 5181–5188.

White, F. M., 2008. *Viscous Fluid Flow.* 2nd ed. New York: McGraw Hill.

Yimin, X. & Qiang, L., 2000. Heat transfer enhancement of nanofluids. *International Journal of Heat and Fluid Flow,* 21(1), pp. 58-64.

Yimin, X. & Qiang, L., 2003. Investigation on Convective Heat Transfer and Flow Features on Nanofluids. *Journal of Heat Transfer,* 125(1), pp. 151-155.

Yu, W., France, D. M., Routbort, J. L. & Choi, S. S., 2008. Review and Comparison of Nanofluid Thermal Conductivity and Heat Transfer Enhancements. *Heat Transfer Engineering,* 29(5), pp. 432-460.